Universidade Nova de Lisboa

Instituto de Higiene e Medicina Tropical

SPORE SURFACE DISPLAY OF ENZYMES USED FOR MOLECULAR DIAGNOSIS BY RT-LAMP

Constança Maria Baptista Machado dos Santos Neves

A THESIS SUBMITTED FOR THE DEGREE OF MASTER IN MEDICAL MICROBIOLOGY

OCTOBER, 2022

Universidade Nova de Lisboa

Instituto de Higiene e Medicina Tropical

SPORE SURFACE DISPLAY OF ENZYMES USED FOR MOLECULAR DIAGNOSIS BY RT-LAMP

Author: Constança Maria Baptista Machado dos Santos Neves

Supervisor: Dr. Mónica Serrano

Co-Supervisor: Dr. Catarina Pimentel; Prof. Dr. Adriano O. Henriques

A thesis submitted to fulfil the requirements for completing the degree of Master in Medical Microbiology

Financially supported by project "STOP-COVID - Strategies to prevent COVID-19 by early detection of asymptomatic carriers at increased risk: epidemiological studies and validation of a rapid in-house diagnostic test"

Acknowledgments

I would like to start by thanking the Scientific Committee of the MSc Medical Microbiology of Instituto de Higiene e Medicina Tropical of Universidade Nova de Lisboa for accepting me in this course, which provided me with diverse knowledge and experience about the scientific world. I also would like to thank the Instituto de Tecnologia Química e Biológica António Xavier of Universidade Nova de Lisboa for receiving me and allowing me to develop my Master's project and make me part of this big scientific family.

With all my heart, I'm deeply grateful to my supervisor Mónica Serrano, who had enormous patience with me, for this was my first time working in a laboratory. For always being there in the good and bad moments, always pushing my capabilities to be a better person, emotionally and in the work. To both my co-supervisors, Adriano O. Henriques and Catarina Pimentel, for opening the door of their laboratories, for showing me to be positive about my results, even when they were not what I desired and for all the knowledge which provided me to think over and beyond.

A special thanks to Khira Amara for her guidance, patience and care. Without her advice, I would take much longer to finish this thesis. To Catarina Amaral and Inês Morais, who help me throughout my work in the laboratory. To all my other MDL colleagues, a very harm hug to Isabel Roseiro, Diogo Martins, Carmen Olivença, Paula Teixeira and Zoé Vaz da Silva. Thank you all for the amazing time I spend with you, making those long working hours feel like a walk in the park. An enormous thank you to General Wilson Antunes, who kindly provided RNA samples for my work in the most crucial time of this thesis. A big thank you to Teresa Silva, for all the help with the solutions, teachings and being the sweetest person of the institute.

To all my friends, from "discórdia" to "weeb kimchi", thank you so much for the support and for the laughs. A special thanks to both of my best friends, Daniela Montean and João Fernandes, for all the late nights talking about our problems and aspirations, reliving my mind and heart.

For last, but clearly not the least, I would like to thank my family. To my mom and dad, who have always encouraged me to be the best of the best and that greatness doesn’t come by itself, you must work hard for it. I hope I make you proud. To my two little gremlins, João and Francisco, who I will always pester no matter how old they have become.

Abstract

The use of enzymes in a wide scale for industrial applications or molecular diagnosis is limited, due to high production and purification costs and often their low stability. This can make access of these enzymes difficult to laboratories with scarce economic resources. Loop-mediated isothermal amplification, or LAMP, is a nucleic acid amplification method developed in the 2000's as a less expensive and simple alternative to PCR, which is widely used in molecular diagnostics. The main enzyme used in LAMP is a DNA polymerase, Bst, from *Bacillus stearothermophillus*. For the detection of pathogens in which RNA is the genetic material, a reverse transcriptase is added to the LAMP reaction (RT-LAMP). LAMP does not require temperature cycling and therefore can be easily implemented in low-resource settings. To make LAMP even more accessible, it would be of interest to develop a platform enabling simple, robust, and inexpensive production and purification of the reverse transcriptase and Bst. This could be achieved by simply displaying the enzymes on the surface of organisms to obviate the need for purification steps, increase their stability and allow their reuse. A well-studied option is the surface of the *Bacillus subtilis* spore, which has been used in the past for the display of enzymes or antigens in view of various biotechnology and biomedicine applications

This study is focused on the display of the RT-LAMP enzymes, Bst and a variant of the reverse transcriptase from feline immunodeficiency virus, MashUp-RT, at the surface of *Bacillus subtilis* spores. Aiming at obtaining a high enzyme concentration and increasing their exposure to the environment, the anchor proteins chosen for this study were CotZ and CotY. Both are abundant components of the crust, the outermost layer of the spore. We were able to display Bst and MashUp-RT at the spore surface, with a minimal impact on the yield of spores, their composition and functional properties. Importantly, we note that when CotZ was used as the anchor, several proteins of the outer coat were absent from spores, suggesting that CotZ is important to maintain the integrity of the outer coat. We also evaluated whether this system could be used to detect the genetic material of pathogens. Only MashUp-RT showed enzymatic activity. Interestingly, although the recombinant spores displaying Bst did not show DNA

polymerase activity, the residual reverse transcriptase activity of the commercial enzyme was stabilized by wild type spores.

To our knowledge, this is the first report on the the use of spore display of enzymes used in molecular diagnostic testing.

Keywords: *Bacillus subtilis*, Spores, Crust, Spore-Display, RT-LAMP

Resumo

O uso de enzimas em larga escala para aplicações industriais ou diagnóstico molecular é limitado devido ao alto custo de produção e purificação e à baixa estabilidade das mesmas. Estas dificuldades limitam a utilização destas enzimas por laboratórios com orçamentos limitados. O LAMP (*Loop-mediated isothermal amplification*) é um teste de amplificação de ácidos nucleicos desenvolvido nos anos 2000 como alternativa mais barata e simples ao PCR na deteção de patogénios, o teste mais utilizado no diagnostico molecular. A principal enzima utilizada no LAMP é a polimerase de DNA Bst do *Bacillus stearothermophillus*. No caso da deteção de patogénios que têm RNA como o seu material genético, é necessário a adição de uma transcriptase reversa à reação de LAMP (RT-LAMP). LAMP não necessita de ciclos de temperatura e por isso consegue ser implementado em laboratórios com poucos recursos. De modo a tornar esta técnica mais acessível, seria de interesse desenvolver uma plataforma simples e robusta para a produção e purificação da Bst e da transcriptase reversa. Esta ideia poderia ser posta em prática com a apresentação destas enzimas à superfície de um organismo de forma a contornar purificações, aumentar a sua estabilidade e permitir a sua reutilização. Uma das opções mais bem estudada são os esporos de *Bacillus subtilis*, que foram usados com sucesso no passado para a apresentação de diversas proteínas à sua superfície com vista a diversas aplicações em biotecnologia e biomedicina.

Este estudo foca-se na apresentação das enzimas utilizadas em RT-LAMP, a Bst e a MashUp-RT, na superfície dos esporos de *Bacillus subtilis*. De modo a obter uma maior quantidade de enzima e aumentar a exposição destas, as proteínas escolhidas como âncora foram CotZ e CotY. Ambas são componentes abundantes da crosta, a camada mais exterior do esporo. Conseguimos apresentar ambas as enzimas à superfície do esporo, com um impacto mínimo no rendimento da produção de esporos e na sua estrutura e propriedades. É importante notar que, quando CotZ foi utilizada como âncora, várias proteínas do manto externo do esporo estavam ausentes, sugerindo que esta é importante para manter a integridade do manto externo. Também foi avaliado se esta metodologia poderia ser utilizada na deteção de material genético de patogénios. Apenas a enzima MashUp-RT apresentou atividade enzimática. Curiosamente, embora os esporos

recombinantes apresentando Bst não mostrassem atividade de DNA polimerase, a atividade residual de transcriptase reversa da Bst comercial foi estabilizada na presença de esporos selvagens.

Tanto quanto sabemos, este é o primeiro estudo sobre a apresentação de enzimas utilizadas no diagnóstico molecular à superfície do esporo.

Palavras-chave: *Bacillus subtilis*, Esporos, Crosta, Display-esporos, RT-LAMP

Table of Contents

Figures Index

Symbols and Abbreviations

%	Percentage
~	Approximately
±	Plus Minus
µg	Microgram
µM	Micromolar
Amp	Ampicillin
Amp^R	Ampicillin Resistance
B&W	Bott and Wilson
bp	Base pair
Cm	Chloramphenicol
Cm^R	Chloramphenicol Resistance
ddH_20	Double Distilled Water
DNA	Deoxyribonucleic Acid
DSM	Difco Sporulation Medium
x *g*	G-force
h	Hours
H_20	Water
IgG	Immunoglobulin G
kb	Kilo Bases
kDa	Kilo Dalton
Km	Kanamycin
LA	Luria Agar
LAMP	Loop-Mediated Isothermal Amplification
LB	Luria Broth
Ib/in^2	Pounds per Square Inch
M	Molar
mg	Milligram
min	Minutes
ml	Millilitre
mM	Millimolar
ºC	Degrees Celsius
OD	Optical Density
OD_{580}	Optical Density at 580 nm
OD_{600}	Optical Density at 600 nm
PBS	Phosphate Buffer Saline
PBS-T	Phosphate Buffer Saline –(Tween)
PCR	Polymerase Chain Reaction
RNA	Ribonucleic Acid
rpm	Rotation per Minute
RT	Reverse Transcriptase
RT-LAMP	Reverse Transcriptase Loop-Mediated Isothermal Amplification
SDS-PAGE	Sodium Dodecyl Sulphate – Polyacrylamide Gel Electrophoresis
SOE	Splicing by Overlap Extension
UV	Ultraviolet
V	Volts

v/v	Volume per Volume
w/v	Weight per Volume
WT	Wild type
Δ	Deletion
σ	Sigma Factor

Chapter 1 - Introduction

1.1 *Bacillus subtilis*, a model organism

The history of microbiology and medicine has always been intertwined. The discovery of the microbial origin of infectious diseases, the formulation of Koch´s postulates and the development of a microbial vaccine by Pasteur, both based on studies with *Bacillus anthracis*, are examples [1]. The genus *Bacillus* includes pathogens but it is also known as including species that are important producer of biopesticides, proteases, antibiotics, vitamins and other compounds with uses in biomedicine and biotechnology [2].

Bacillus subtilis is a Gram-positive, aerobic endospore-forming organism. Although this rod-shaped bacterium is normally viewed as soil dwelling, it can also be found in the gastrointestinal tract of several animals, including humans [3]. It belongs to the Firmicutes phylum, alongside with other endospore-formers like *B. cereus*, *B. anthracis* and *Clostridioides difficile*. *B. subtilis* was first described by Ferdinand Cohn in the 19th century [4]. In 1997, the genome sequence of *B. subtilis* strain 168 was published, providing a greater insight to its genetic organization and stimulating even further research in what was already an intensely studied organism [5]. The impressive toolbox of techniques for its genetic manipulation have established *B. subtilis* as a model organism for studies on all aspects of Biology, but in particular on studies of cellular development, including biofilms and spore morphogenesis [5, 6].

The dormant endospore (hereinafter spore for simplicity) is highly resistant to a wide range of chemical and physical stresses. The assembly and structure of the spore surface has been intensely studied. The Food and Drug Administration (FDA) classifies *B. subtilis* as a GRAS (generally recognized as safe) organism. These circumstances have prompted many applications of *B. subtilis* spores in biotechnology and biomedicine. The use of the spore surface, in particular, for the display of foreign proteins, is one such application that we have exploited in this work. This family of applications bypasses the need for the often time consuming and expensive steps of protein purification.

1.2 Sporulation in *B.subtilis*

1.2.1 Overview of sporulation

Since sporulation is a prolonged and energy-consuming process, *B. subtilis* will only embark in this developmental process leading to spore formation as a last-resort survival adaptation [7]. When facing extreme nutrient deprivation, *B. subtilis* will switch to the sporulation pathway by first replicating its chromosome; then, the rod-shaped cell divides asymmetrically, creating two daughter cells, the larger mother cell and the smaller forespore, each with one copy of the genome (Fig. 1A) [7]. The mother cell will help in the morphogenesis of the spore, while the forespore will become the mature spore. In a mechanism analogous to phagocytosis, the mother cell will engulf the forespore, isolating this cell from the external medium. [7, 8]. Following engulfment completion, the sporulating cell enters the final stages in the assembly of the spore protective layers, the spore cortex peptidoglycan and the protein coat around the developing spore. The assembly of these two layers is mainly a function of the mother cell [7, 8]. At the end of the process, the mother cell lysis and the mature spore is released into the environment.

Even though spores are dormant, they are able to sense their surroundings and once they perceive environmental conditions able to support growth and survival of the organism, they will germinate into vegetative cells [9].

1.2.2 Sporulation regulatory network

During sporulation, gene expression is regulated by sporulation specific RNA polymerase sigma factors: σ^F, σ^E, σ^G and σ^K [10]. These sigma factors are activated in a cell type-specific manner at different sporulation stages and in response to morphogenic cues. After the formation of the asymmetrical septum and prior to engulfment completion, σ^F and σ^E regulate gene expression in the forespore and mother cell, respectively (Fig. 1A) [11]. At late stages, following engulfment completion, σ^G and σ^K replace σ^F and σ^E, respectively (Fig 1A) [10]. The gene expression during sporulation is further controlled by accessory transcription factors: SpoIIID, GerR, GerE, RstA and SpoVT [10, 12, 13]. σ^E turns on the expression of the genes encoding for GerR and SpoIIID. GerR is a transcriptional repressor down-regulating many σ^E dependent genes. SpoIIID acts as a repressor but also as a transcription activator of some σ^E dependent genes, including the ones involved in σ^K production and activation. σ^K turns on the expression of the gene

coding for GerE. This transcriptional regulator acts both as a repressor and an activator of the σ^K- dependent genes. This tight regulation of gene expression in the mother cell is important for the correct assembly of the protective layers around the forespore [10].

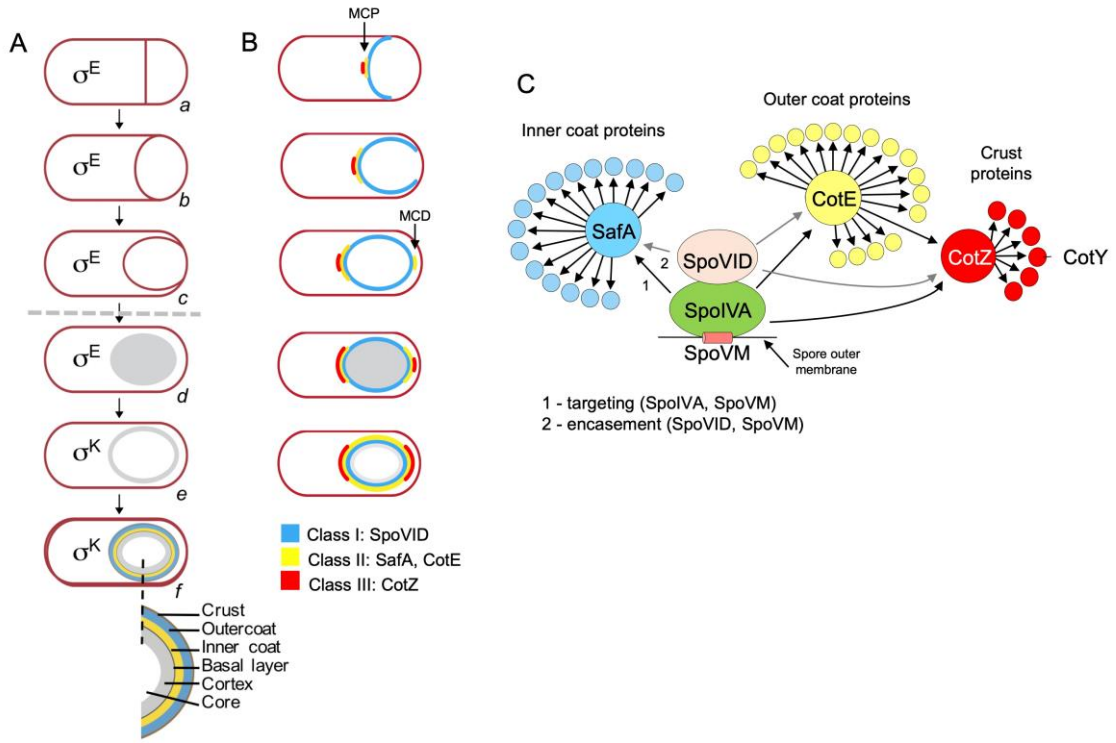

Figure 1. *Bacillus subtilis* sporulation cycle and early encasement classes. A) Mother cell specific sigma factors that govern progress through sporulation. Sporulation starts with the creation of an asymmetric septum (a). σ^E is activated in the mother cell, regulating gene expression prior the engulfment of the forespore (a-d). When engulfment ends, σ^K replaces σ^E (e), activating a late set of mother cell-specific genes. The assembly of the protective layers around the spore is manly a mother cell function (f). **B)** Encasement classes are based on the localization patterns of coat proteins. The early classes (I, II and III) localize early, before engulfment completion, in the mother cell proximal (MCP) pole. After engulfment is completed these proteins localize at the mother cell distal (MCD) pole. At the end the coat proteins form a complete shell around the forespore. **C)** coat proteins regulatory network. SpoIVA needs SpoVM and SpoVID for its recruitment on the spore outer membrane. This morphogenetic protein recruits SafA, CotE and CotZ, which are responsible for the inner layer, outer layer and crust assembly respectively. The CotZ also requires the CotE for its recruitment. SpoVID is also responsible for the encasement of these proteins. Adapted from [14] and [15].

In the forespore, *rsfA* expression is under σ^F control and RsfA act as a repressor of gene expression in this cell. σ^G activates the expression of the gene coding for SpoVT, which act as an activator and a repressor of some genes that had been turned on by σ^G and

σ^F[16]. The forespore line of gene expression includes mainly genes that contribute to the resistance and germination properties of the spore [13].

Spo0A is the main regulator in the entry of sporulation and is activated by phosphorylation before asymmetric division. Four sensing kinases (KinA, KinB, KinC and KinD) act directly on Spo0A, or indirectly via a phosphorelay involving Spo0F and Spo0B, and these proteins determine the cell concentration of Spo0A-P [13]. High levels of Spo0A-P are necessary to activate the transcription of various key sporulation-specific genes, specifically *spoIIA*, coding for σ^F, *spoIIE,* required for σ^F activation and *spoIIG*, coding for σ^E [17]. In such manner, the genes coding for σ^F and σ^E are transcribed before the formation of the asymmetrical septum but σ^F and σ^E and are held inactive until cell division. After this, σ^F will become active in the forespore, triggering a signal transduction pathway for the activation of σ^E in the mother-cell [17]. As mentioned before, both factors will promote the synthesis of σ^G and σ^K respectively, in their respective cells. However, σ^G and σ^K are kept inactive until completion of the engulfment process. Late gene expression in the forespore requires σ^E expression in the mother cell, while σ^K is activated by a signal generated in the forespore under the control of σ^G [18]. Therefore, the two cells communicate with each other through signalling pathways, that function at key morphological stages.

1.2.3 Endospore structure and properties

Spores are dormant and highly resistant cells with extreme longevity, allowing for the dispersal of bacteria throughout different environments [19]. The resistance of spores to physical-chemical and biological factors such as heat, ultra-violet (UV) radiation, solvents, lytic enzymes, oxidizing agents and predators, are directly associated with their multiple layers and their assembly [8].

Even though there is a large diversity of spore-formers, the basic spore architecture is conserved across species [12]. The structure consists of a series of concentrically arranged layers that have the role of protecting the bacterial genome localized in the central core (Fig. 1A). [8]. The core is surrounded by a membrane, followed by the germ cell wall, which will become the cell wall of the cell that outgrows from germinated spores. Surrounding the germ cell wall is the cortex, a modified peptidoglycan layer responsible for the dehydration, mineralization and dormancy of the

spore, resulting in its thermo-resistance [12]. Surrounding the cortex is the spore coat, consisting of three main sub-structures: the inner lamellar coat, the electrodense outer coat and the crust (Fig. 2A). The coat is important for the resistance of the spore against lytic enzymes such as host-produced lysozyme, solvents, UV radiation and predators [12]. The crust mediates adhesion to surfaces and confers hydrophobicity; it influences the interaction between spores with the surrounding environment [20].

Although not present in the *B. subtilis* spore, in many pathogenic species there is an outermost structure, the exosporium [12]. This layer is also composed of glycosylated proteins, similarly to the *B. subtilis* crust, and is the first line of contact of the spore with the host cells and the environment [21].

1.2.4 Coat assembly

Coat assembly is controlled by the mother cell-specific transcriptional cascade and several post-translational processes, including the action of assembly guides known as morphogenetic proteins. Coat proteins are initially targeted to the spore surface and then encase the developing spore. Targeting depends mainly on the SpoIVA and SpoVM proteins, whereas encasement relies mainly on the SpoVID protein (Fig. 1C). SpoVM is small, 26-residues long protein that recognizes positive curvature and localizes to the forespore outer membrane [22, 23]. SpoIVA is an ATPase that directly interacts with SpoVM and polymerizes in an ATP-dependent manner to form cables along the forespore surface. These cables form the basal layer upon which the coat is assembled.

Coat proteins can be distributed in six classes based on localization patterns and kinetics of encasement [24]. After production in the mother cell, most coat proteins localize in two steps. First in the mother cell proximal (MCP) pole of the forespore, facing the mother cell cytoplasm, followed by localization in the mother cell distal (MCD) pole. At the end the coat proteins localize in a complete circle around the forespore (complete spore encasement). Kinetics class I, II and III (Fig. 1B) include proteins that are produced before engulfment under the control of σ^E. Classes IV, V, and VI include proteins produce after engulfment completion under the control of σ^K. Proteins from the first three classes localize simultaneously to the forespore surface but complete encasement at different times, coincident with the last three classes: class I and IV proteins complete spore encasement just after engulfment completion; class II and V proteins complete

encasement during cortex synthesis; and class III and VI during the late stage of spore cortex synthesis, when the spore becomes phase bright.

As mentioned above, the initial localization and encasement of the coat proteins is controlled by three class I morphogenetic proteins: SpoIVA, SpoVM, and SpoVID (Fig- 1C) [24]. Class II morphogenetic proteins SafA and CotE control the assembly of the inner and the outer layer, respectively [24]. Three proteins from the class III (CotX, CotY, and CotZ) are required for crust formation [24]. The coat interaction network follows a hierarchy, represented in figure 1C: as mentioned above SpoIVA is required for the initial targeting of the coat proteins to the forespore surface; SpoVM and SpoVID are required for encasement. Initial localization of the morphogenetic proteins SafA and CotE is dependent on SpoIVA and SpoVID and localization of CotX, CotY, and CotZ is dependent on CotE. In addition, each morphogenetic protein that drives assembly of the coat sub-layers is thought to interact with several structural coat proteins therefore functioning as hubs [22, 24]. One aspect to take note is the continuous addition of proteins belonging to internal layers after the morphogenic proteins of the same layer have already finished their encasement. This is important for the later classes, since they include proteins from all the layers of the coat, suggesting some sort of permeability that allows the access of late expressed proteins [24].

1.2.4 Crust layer

The crust, the most external coat layer, contains at least six different proteins, CotV, CotW, CotX, CotY, CotZ and CgeA, interacting and stabilizing each other in a complex network [8]. The crust genes *cotVWXYZ* are clustered together, organized in three transcriptional units (*cotVWX*, *cotX* and *cotYZ*) all under σ^E and σ^K control (Fig. 2B) [20, 25]. The *cgeAB* operon is localized on another chromosomal location and expressed under σ^K and GerE control [26].

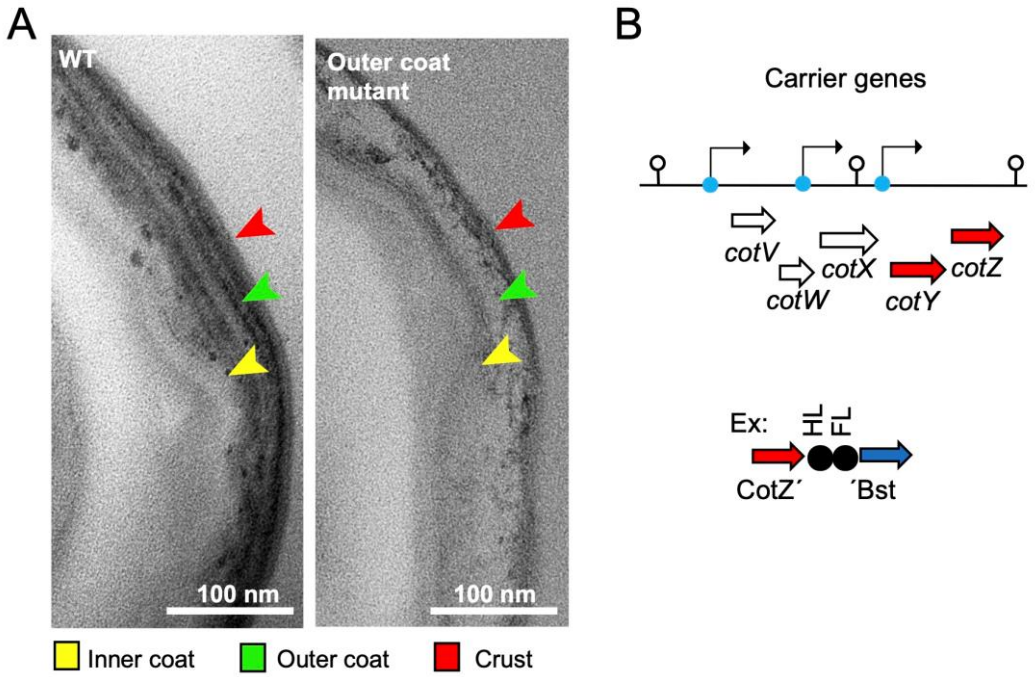

Figure 2. *Bacillus subtilis* spore crust. A) Electron microscopy of a thin section of a *B. subtilis* spore. The inner coat (yellow arrows), the outer coat (green arrows) and the crust (red arrow) are indicated. The crust layer is easily recognized in the right panel that show a spore in which the outer coat is absent (*cotG* mutant). Adapted from [27]. **B)** operon structure of the region of the *B. subtilis* chromosome carrying the crust genes. The P_{cotVWX} promoter is under the control of σ^K and GerE, regulating the expression of the crust genes *cotV*, *cotW* and *cotX*. The latter is also under the control of the P_{cotX} and can thus be expressed independently. The *cotY* and *cotZ* genes are regulated by the P_{cotYZ} promoter, which is under the control of σ^E, at the beginning of the sporulation, and of σ^K and GerE in later stages of the process. In the bottom a schematic representation of a fusion protein produced in this study, where the linker used is composed of a sequence that forms a short, rigid α-helix (HL), followed by a sequence which assumes a flexible conformation (FL).

CotV, CotX, CotY and CotZ possess glycosylation domains, which agrees with the observations that the crust is a glycoprotein layer, based on its staining by ruthenium red. CotY and CotZ, the most abundant components of the crust, are cysteine-rich proteins with self-assembly ability through the cooperative formation of disulphide bonds [26, 27]. CotZ acts as an anchoring for the other crust proteins. CotW, CotX and CotV are minor components of the crust and are co-dependent on each other for their localization [26, 27]. CgeA is implicated in the glycosylation of the crust proteins and depends on the other crust proteins for its localization [20].

The crust, as the spore outermost layer, has great potential for the display of foreign proteins.

1.3 Protein Surface Display

1.3.1 Methods for displaying proteins

Proteins used in diagnostic with biotechnological and biomedicine application are often targets for engineering with the aim of increase their stability, substrate affinity and catalytic activity [29]. One way to achieve this goal is to display proteins of interest onto biological surfaces, like phage, yeast, bacteria and mammalian cells and also bacterial spores. All of these methods include a carrier protein, which anchors the protein of interest, the passenger protein, to the surface of the cell or cellular structure [30]. To minimize the interaction between this carrier and the protein to be displayed, a peptide flexible linker is often included between the two.

In phage display, the gene encoding the protein of interest is inserted in frame with a gene coding for a phage coat protein, which is then expressed as a fusion protein when the phage infects a host cell [31]. After the assembly of the phage components, the protein fusion is displayed at the surface of the bacteriophage. In comparation with the yeast and mammalian cells, bacterial libraries hosting phages are usually cheap and easy to grow [32]. In terms of disadvantages, folding errors and expression bias are a common occurrence, making it difficult to express large proteins, not to mention the fact that there is a great diversity of libraries with a low concentration of the displayed protein [33].

In display strategies with bacteria or yeasts cells, the carrier is a cell surface protein possessing a signal sequence, allowing transport of the fusion protein to the cell surface, where it will be immobilized and exposed to the outside [30]. However, this strategy is far from perfect: posttranslational modifications may occur; there are mass transfer limitations; enzymes may be inactivated during transport; proteins can be incompletely exposed; and the substrate may become inaccessible to the enzyme [34].

1.3.2 Spore Display

As mentioned above, *B. subtilis* spores are an extremely stable and resistant. In addition, the large number of possible carrier proteins available at different levels of the structure and the knowledge that has been accumulated of the coat/crust assembly process, make the spore surface a versatile platform for protein display. For the spore display of proteins, two methodologies have been applied: a non-recombinant display system, in

which proteins or other molecules are non-covalently adsorbed onto the spore surface (spore absorption), and a recombinant system [35]. The spore absorption system does not require the genetic manipulation into the spore coat assembly pathway since it is based on direct adsorption of purified proteins on the spore surface [35]. In a study in which β-galactosidase was adsorbed to spores, this enzyme showed similar kinetic proprieties but enhanced resistance proprieties, such as thermo-resistance and resistance to low pH, when compared to its free version [36]. This shows that the spore can act as a stabilizer for the displayed enzyme, protecting it from harsh conditions. In another example, the heat labile toxin (LTB) of *E. coli* was absorbed to the *B. subtilis* spores in its oligomeric form (a pentamer), in contrast to what happens when displayed as a fusion with a coat protein where only monomers could be displayed [37]. Nonetheless, one of the major downsides of the system is the non-selective absorption to the spore [38], and the requirement for enzyme purification before absorption. Variations of this technology include the use of heat-inactivated spores or the production of the protein to be adsorbed during the sporulation process, but not as a fusion to a coat protein [35]. These approaches, however, require the use of recombinant cells.

In the recombinant system the display is achieved by fusing the gene coding for the protein of interest to a gene that codes for a coat or crust protein. At the end of the sporulation process the spores formed will have assembled the recombinant protein onto the coat layers [39, 40]. The coat carrier protein should be abundant and its location must allow for target protein contact with the external environment, if that is the goal. However, if the goal is for the spores to be ingested, more internal locations, giving greater protection during transit through the gastro-intestinal tract may be desirable [39]. Two successfully used carrier proteins are CotY and CotZ, which, as mentioned above, are abundant proteins located at the outermost layer; importantly, spore formed by *cotYZ* mutants do not show sensitivity to lysozyme or heat which is an advantage in case the fusion perturbs the function of the native proteins [26]. Compared with the previous systems, this one has several advantages, such as high protein stability even after prolonged storage, the ability to display large multimeric complexes, minimal disturbance of the spore structure, the absence of codon bias and no requirement for the fusion protein to be transported across a membrane, since it is produced alongside with the coat proteins in the mother cell cytoplasm and assembled around the spore [41]. Moreover, depending

on the endogenous carrier, the abundance of the displayed protein can be very high, even if the efficiency of the process is somewhat compromised by the fusion [41, 42]. The limitations of this methodology are mainly the possibility the inactive enzymes are produced, the concentration of displayed protein around the spore and characteristics of the carrier protein such as stability and distribution around the spore [30, 41].

One interesting way to merge both display systems was used in the study by Long Chen in 2016, where a protein from the outer coat (CotG) was fused to dockerins, which interact with immobilized cohesins fused to specific enzymes, creating a covalent bond[43]. A limitation of this approach is the need for production and purification of recombinant proteins and the possible interference of cohesin on the folding and function of the enzyme.

1.4 Molecular Diagnosis of pathogenic diseases

There are a number of options available for the molecular detection of infectious agents or diseases [44]. They are generally based on nucleic acid amplification (NAATs), of which the polymerase chain reaction (PCR) stands out as the gold standard method for detecting most pathogens [45]. Although very sensitive, PCR is not perfect, demanding the use of specific and expensive equipment, trained personnel, multiple protocols and long turnaround time for results [46].

1.4.1 LAMP and RT-LAMP

Loop-Mediated Isothermal Amplification (LAMP) developed by Notomi *et al* in the 2000's, has emerged as an equally sensitive alternative to PCR[47]. It is a fast and low-cost method that doesn't require special equipment and facilities, is highly sensitive, and easily deployable due to its simplicity [46, 47].

The LAMP reaction runs at a fixed temperature, typically 65 ºC, and takes only 30 min to complete [50]. In its simplest format, it does not require thermocyclers or fluorimeters and a heat block or water bath is sufficient to carry out the reaction. LAMP requires at least 2 inner (FIP and BIP) and 2 outer (F3 and B3) primers, which recognise a specific region of the target gene (Fig. 3). Nonetheless, the most common practice for improving and accelerating the amplifications is to use 3 pairs of primers; the FIP/ BIP, F3/B3 and 2 more loop-specific primers (LF and LB) (Fig. 3)[48]. The amplification is

catalyzed by a DNA polymerase from *Bacillus stearothermophillus* (Bst), leading to the formation of a stem-loop DNA-structure, which is the template for the exponential amplification [51]. Whenever the target genetic material is RNA, a reverse transcriptase (RT) needs to be added the reaction, which is then called reverse-transcription loop-mediated isothermal amplification (RT-LAMP).

There are multiple ways to analyse the LAMP reaction products. Among them are agarose gel electrophoresis, UV-light illumination, real-time fluorescence or end-point colorimetric readouts [52]. The colorimetric format of LAMP is based on the detection of the reaction by-products, protons or pyrophosphate, released when deoxynucleotide triphosphates are incorporated into newly synthetized DNA [53–55]. In the presence of a complexometric or pH-sensitive indicator dye, a colour change occurs in positive cases. The most widely used pH-sensitive dye is phenol red which is assembled with the other components of the reaction; acidification of the reaction during DNA amplification induces a colour shift from pink to yellow, indicating the presence of target RNA/DNA. LAMP, in particular the colorimetric format, represents a major advantage since it eliminates the need for sophisticated and expensive equipment required for amplification and detection and can therefore be easily deployed at the point of care [56].

Recent studies have proven the effectiveness of LAMP in the diagnosis of pathogenic diseases such as those caused by SARS-CoV-2 [54, 55], human T-cell lymphotropic virus type 1 (HTLV-1) [58], *Leishmania* sp. [59] and *Mycobacterium leprae* [60].

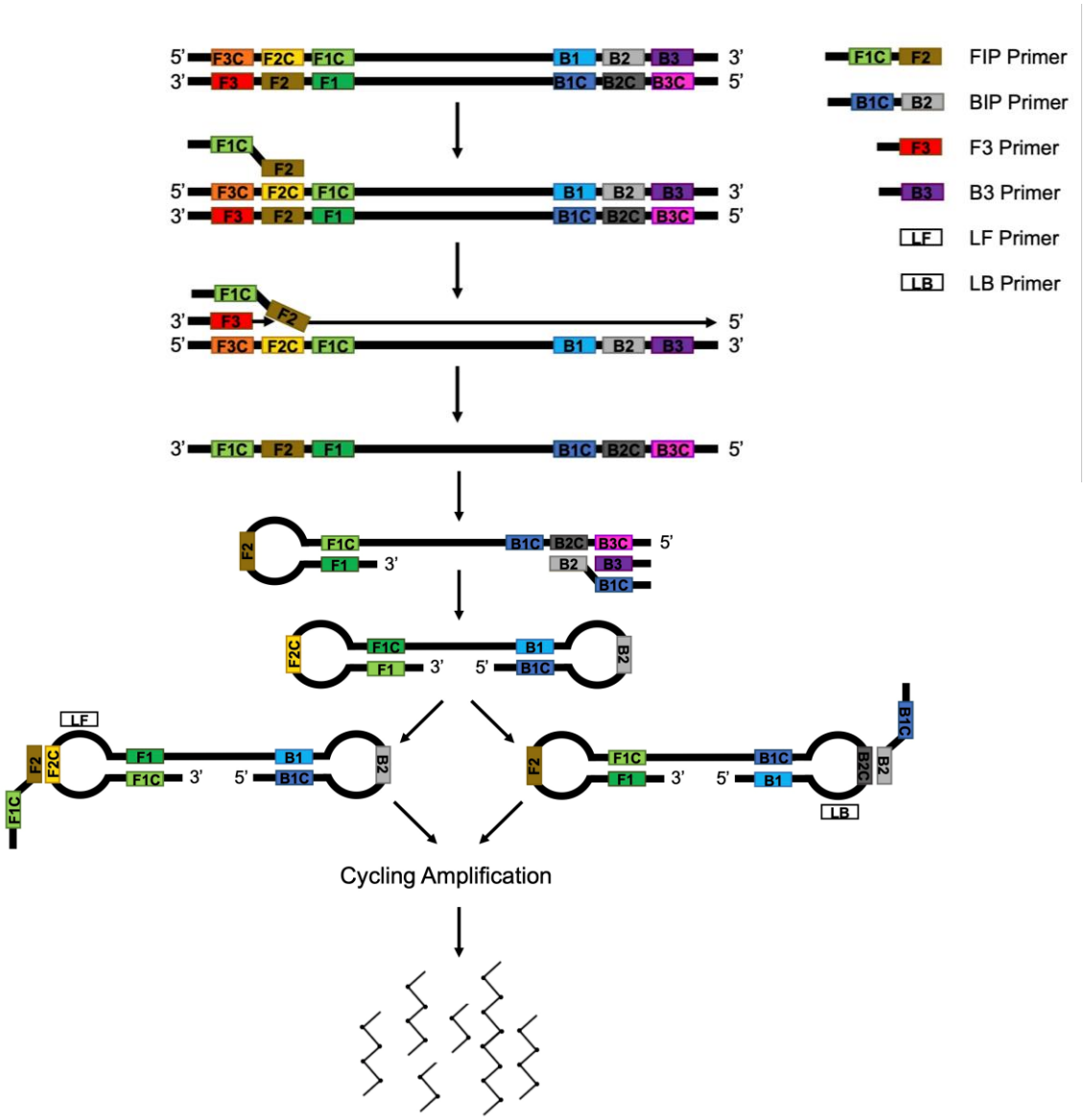

Figure 3. Loop-Mediated Isothermal Amplification (LAMP) reaction. The inner primer FIP contains the regions F2 (brown square) and F1C (dark-green square). FIP hybridizes with the F2C (yellow square) region on the target DNA, starting the amplification. The outer primer F3 anneals with the regions F3C (orange square) of the target DNA, resulting in the replacement and release of the strand elongated from FIP, forming a loop structure at its 3' end. Next, the inner primer BIP, which contains regions B2 (light-grey square) and B1C (dark-blue square), will anneal with the region B2C (dark-grey square). The outer primer B3 anneals with B3C (pink square) and much like F3 and FIP, resulting in the displacement of the DNA strand and in a loop at the 5' end. A dumbbell DNA structure is formed that will be used as a template for the cycling amplification, resulting in long DNA structures. The additional primers LF and LB may also be used to accelerate the amplification process. Adapted from [47].

1.5 Aim of this study

Rapid diagnosis of pathogenic infections is essential to enable timely therapies and prevent the spread of diseases in the community. Molecular diagnosis techniques, such as LAMP and RT-LAMP, can advance infectious diseases diagnosis with minimal requirements of equipment. However, the enzymes used in these assays are very sensitive to factors such as temperature and are high costly to produce and purify, leading to high market prices. Several studies have shown that it is possible to successfully display proteins and enzymes on the surface of *B. subtilis* spores [39, 59, 60], eliminating the need for protein purification. The major goal of this thesis was to display the enzymes used in LAMP and RT-LAMP on the surface of *B. subtilis* spores, to set up a "low-cost" platform for LAMP-based molecular diagnosis.

The specific objectives of this study were to:

1. Create *B. subtilis* strains expressing fusion proteins Bst and MashUp-RT to crust proteins CotY and CotZ;
2. Characterize the spores displaying the fusion proteins;
3. Test the spores displaying Bst in LAMP reactions;
4. Test the spores displaying MashUp-RT in RT-LAMP and RT-PCR reactions.

Chapter 2 – Materials and Methods

2.1 Microbiological techniques

2.1.1 Bacterial strains and general growth conditions

The *B. subtilis* strains used in this work, are congenic derivatives of the WT strain PY79 [62]. The *Escherichia coli* strain DH5α (Invitrogen) was used for molecular cloning and BL21(DE3) (Novagen) was used for protein over-production. Strains were stored at -80 ºC in 15% glycerol. All bacterial strains are listed in Annex 6.1. Cells were routinely grown in Luria Broth (LB); LB plates were prepared by adding agar to 1.5% (wt/vol). Liquid LB or plates were supplemented with the appropriate antibiotics when needed. All growth media and solutions used in this work are listed in Annexes 6.4 and 6.5, respectively.

2.1.2 Spore production and purification of spores

For spore production, a pre-inoculum was made by growing cultures for 5 h at 37 ºC with orbital shaking in LB medium supplemented with the appropriate antibiotic(s). After this time, 1 mL of this culture was transferred to 100 mL of Difco Sporulation Medium (DSM; DIFCO) supplemented with 1 mM $Ca(N0_3)_2$, 0.01 mM $MnCl_2$ and 1 μM $FeSO_4$, and the resulting culture was grown under the same conditions for 24 h [63]. Following this, the culture was centrifuged at 4 ºC at 7519 x*g* for 10 min, and the sediment was resuspended in 100 mL of cold (4 ºC) ddH_2O. This suspension was then left at 4 ºC for at least 24 h. After this period, the suspension was again centrifuged in the same conditions as before, and the sediment was resuspended in 1 mL of a 20% (v/v) solution of metrizoic acid (Gastrografin, Bayer). This new suspension was layered on top of a 50% (v/v) solution of Gastrografin and then centrifuged for 30 min at 4 ºC, 7519 x*g*. The spores at the bottom were resuspended in 1 mL of cold ddH_2O and washed 5 times to remove all of the remaining Gastrografin and stored at -20 ºC. Spores were quantified by measuring the optical density of the suspension at 580 nm (OD_{580}).

2.1.3 Sporulation assays

For sporulation assays the strains were grown as described above (2.1.2). After 24 h, serial dilutions in B&W salts were made and 100 μL of the 10^{-4}, 10^{-5} and 10^{-6} dilutions

were spread onto LB plates to determine the number of colony forming units (CFU/mL). To calculate the heat-resistant spore titer, the same of dilutions were incubated at 80 ºC for 20 min, and then 100 µL of each were spread onto LB plates. For lysozyme-resistant tests, 250 µL of lysozyme (10 mg/ml) was added to 1 mL of DSM culture and incubated at 37 ºC for 20 min. After this, the culture was centrifuged at 2325 x*g* for 5 min and the supernatant was discarded. The sediment was resuspended in 1 mL of B&W salts, serial dilutions were prepared and 100 µL of the 10^{-4}, 10^{-5} and 10^{-6} were plated onto LB agar. The plates were incubated overnight at 37 ºC. Counting of the CFUs was done manually on the next day.

2.1.4 Auto-induction of protein over-production in *E. coli*

E. coli BL21(DE3) cells carrying the recombinant plasmids were grown in 100 mL of auto-induction medium supplemented with the required antibiotics with orbital shaking at 37 ºC for 18 h before being harvested by centrifugation and the sediment stored at -20 ºC [64].

2.1.5 BATH assays

To test the hydrophobicity of spores, the Bacterial Adherence to Hydrocarbons Assay (BATH) was applied to purified spores [65]. The OD_{600} of a spore suspension diluted in 1:200 in ddH_2O was measured to calculate the amount of spores to be used in 5 mL of PBS 1x to obtain an OD_{600}~0.5. The OD_{600} of 1mL of this solution was measured, indicating the time point A_0 (before hexadecane treatment). Then, a 1 mL aliquot were added into three glass test tubes, labelling them with their respective time points in seconds (A_{30}, A_{60}, A_{90}). To each tube, 500 µL of Hexadecane (Sigma) was layered on top of the spore solution, followed by vortexing for their respective time periods and settle for 30 min. After this time, the OD_{600} of the aqueous layer of each tube was measured and the percentage of spores remaining in this layer was calculated with the formula: $(A_x/A_0)*100$.

2.2 Biochemical Techniques

2.2.1 Spore Coat extraction

Spore coat proteins were extracted from purified spores by boiling the suspension for 8 min in 2x SDS-PAGE loading buffer. To estimate the volume of purified spores to be loaded per well to the 15% SDS-PAGE, the OD_{580} of a spore suspension diluted in 1:200 in ddH_2O was measured and the following formula applied: μL/well: 3600/(OD_{580}*200). The gels were stained with 0.1% (w/v) Coomassie blue or used for immunoblot analysis (see below).

2.2.2 Whole cell extracts from sporulating cells

To prepare protein extracts from sporulating cells the strains were grown as described above (2.1.2). At 4, 6 and 8 hours after the onset of sporulation, 10 ml samples were collected by centrifugation at 7500 ×*g* for 10 min at 4 °C. Cells resuspended in French press buffer were lysed in a French pressure cell at 900 lb/in2. Total protein present in the extracts was quantified using the Bradford protein assay (Bio-Rad Protein Assay). 20 μg of protein was loaded in the SDS-PAGE gels.

2.2.3 SDS-PAGE and Immunoblot analysis

Proteins in the samples were resolved in SDS-PAGE gels (15% or 12.5%) at 40 mA per gel, using the Mini-Protean Cell system (Bio-Rad). The molecular size marker used was the Precision Plus Protein™ All Blue Ladder (BioRad). The gels were stained for 30 min in a Coomassie solution and after transferred to a destaining solution that was changed from time to time until the gel was clear and the protein bands clearly visible.

For immunobloting, proteins in the gels were transferred to a 0.2 μm nitrocellulose membrane in cold transfer buffer for 90 min at a constant voltage of 100 V. Next, the membranes were incubated in 45 mL of blocking solution for 1 h at room temperature with agitation. After this, the blocking solution was removed and the membrane was washed with 10 mL of PBS-T. An anti-His_6Tag antibody (Novagen) was added at a 1:1000 dilution in 10 mL of PBS-T with 0.5% milk (w/v) and the mixture was incubated overnight at 4 ºC with shaking. On the following day, the membrane was washed again with 10 mL of PBS-T. A mouse peroxidase-conjugated secondary antibody (Sigma) was added to 10 mL of PBS-T with 0.5% milk (w/v) at a dilution of 1:5000 and incubated for

30 min. After 3 further washes of 10 min each at room temperatures with agitation, the membrane was developed with Super Signal™ Pico Plus Chemiluminescent Substrate (Thermo Scientific) following the manufacturer's instructions, and the signal recorded using a iBright Imaging System (Invitrogen).

2.2.4 Protein Purification

The cell sediment resulting from the auto-induction procedure were resuspended in 1mL of buffer A and passed through a French Press at 900 lb/in2. After centrifugation, the supernatant was applied to a 1 ml column (MoBiTec) loaded with a Ni^{2+} Sepharose™ High Performance matrix (Cytiva) that had been equilibrated with buffer A. The protein was eluted in buffer B with a step gradient of imidazole (40 mM, 100mM, 300 mM and 500 mM) and collected in 1 mL fractions. The fractions containing the proteins were identified by 12.5% SDS-PAGE. The column was regenerated by washing it with 10 mL of buffer A, sealed and stored at 4 ºC.

2.3 Molecular biology techniques

2.3.1 Plasmid constructions and transformation in *E. coli*

Amplification of the desired DNA fragment was obtained by Polymerase Chain Reaction (PCR) using the Phusion DNA polymerase (Thermo Fisher Scientific). The reaction conditions were established depending on the size of the product, the melting temperature of the oligonucleotides and the manufacturer's indications for the DNA polymerase. The primers and plasmids used in this study are listed in the Annex 6.2 and 6.3, respectively. The purification of the PCR was done using the NZYGelpure (Nzytech). For cleavage of DNA digestions, the restriction and modification enzymes used were from Thermo Fisher Scientific and New England BioLabs, following the companies' respective guidelines. The inserts in all the constructed plasmids were verified by DNA sequencing.

2.3.2 DNA electrophoresis

After adding Orange G loading buffer to the DNA samples, these were subjected to electrophoresis in 1% (w/v) and 2% (w/v) agarose gels in TAE 1X buffer. Gels were run at a constant voltage of 120 V, stained with ethidium bromide (0.001% (v/v)),

visualised under UV radiation of low wavelength and an image was acquired. A 1 kb plus DNA ladder (Invitrogen) was used as molecular weight marker.

2.3.3 Preparation of *E. coli* competent cells

For the development of chemically competent cells of *E. coli*, the $CaCl_2$ method was used [66]. Briefly, *E. coli* was inoculated into LB and incubated at 37 ºC until an OD_{600} of approximately 0.6 is reached. Cells were harvest by centrifugation at 7519 x*g*, 4 ºC for 2 min and the sediment resuspended in cold solution of 0.1 M $CaCl_2$ and incubated in ice for 1 h. After new centrifugation the cells were resuspended in 0.1 M $CaCl_2$ with 15% glycerol and distributed in aliquots of 150 µL. Competent cells were stored at -80 ºC until use.

To transform the competent *E. coli* cells, the cell suspension was incubated for 30 min on ice in the presence of either 1 µL of plasmid DNA or 10 µL of a ligation mixture. A heat-shock of 90 sec at 42 ºC was applied to the cells, followed by incubation of 2 min in ice. Then, 1 mL of LB medium was added and the cell suspension incubated at 37 ºC, with orbital shaking for 1 h. After centrifugation, 900 µL of media was removed, and the cell sediment was gently resuspended in the remaining volume. Finally, the suspension was plated onto LB plates supplement with the required antibiotics.

2.3.4 Extraction of plasmid DNA from *E. coli*

Single colonies of *E. coli* DH5α were grown overnight in LB medium supplemented with the necessary antibiotics. The culture was centrifuged at 16200 x*g* for 7 min, removing the supernatant and resuspending the sediment in a cell lysis solution consisting of 350 µL STET buffer, 0.6 mg/mL Lysozyme and 0.25 mg/mL RNase A, followed by incubation at 37 ºC for 30 min. To denature the chromosomal DNA, the tubes were boiled at 100 ºC for 1 min. After another centrifugation, as above, the cell sediments were removed and the DNA was precipitated by adding isopropanol of 70% (v/v) followed by centrifugation of 30 min, at 4 ºC and 16200 x*g*. Immediately after, the supernatant was discarded, and the sediment was dried at 60 ºC for 10 min to remove the remaining isopropanol. Lastly, the dried sediments were resuspended in 20 µL of ddH_20 and stored at -20 ºC.

In case of highly pure plasmid DNA, the NZYMiniprep (NZYtech) was used in accordance with the instructions provided by the manufacturer.

2.3.5 Competence development and transformation in *B. subtilis*

B. subtilis was inoculated into 5 mL of Growth Media 1 (GM1) and incubated at 37 ºC with orbital shaking for 5 h. Next, 1 mL of GM1 culture was diluted in 4 mL of Growth Media 2 (GM2) and incubated in the same conditions as before for 2 h. For the transformation, 20 µL of plasmid DNA was added to 500 µL of competent cells, followed by a period of incubation of 1 h in the same conditions. Lastly, 200 µL of the transforming mixture was plated onto LB plates supplemented with the necessary antibiotics and the plates incubated at 37 ºC overnight.

To verify if the transformation was successful, two strategies were applied, depending on whether the plasmid DNA was inserted by Campbell recombination or by double crossing-over at the *amyE* locus [67]. On the first case, the *B. subtilis* colonies were submitted to a colony PCR utilising DreamTaq DNA polymerase (ThermoFisher); in this method, a small portion of one colony is mixed with 100 µL 5% (w/v) Chelex (Sigma-Aldrich) and incubated at 95 ºC for 10 minutes. This resin allows the binding of cellular polar components, while RNA and DNA remain in the supernatant. After a centrifugation of 1 min at 2325 x*g*, 2 µL of the supernatant were used for PCR. The positive colonies would be chosen if the PCR amplified a fragment with the expected size. The second strategy is based on the non-essentiality of the *amyE* locus, coding for a secreted α-amylase, where DNA insertions can be easily obtained by double a cross-over event. Here, the *B. subtilis* colonies were submitted to a α-amylase test, where colonies would be streaked on LB plates supplemented with 1% (w/v) starch. Following overnight incubation at 37 ºC, a solution containing 1% (w/v) I_2 and 10% (w/v) KI was added to the plates, to reveal positive colonies, *i.e.*, those not showing a bright halo resulting from starch degradation.

2.3.6 LAMP and RT-LAMP enzyme assays

For Loop-mediated Isothermal Amplification (LAMP) DNA of *Candida albicans* was amplified using 5 primers, which anneal in seven conserved regions within the sequence of internal transcribed spacer 2 (ITS2) [50]. LAMP reaction was performed in a total volume of 20 µL containing 2 µl of template DNA (100 ng/µL 25 pg/µL), 1x mix (1.6 µM Ca_FIP/BIP primers, 0.4 µM Ca_LB primer, 0.2 µM Ca_F3/B3 primers, 1.4 mM each dNTP), 1x Isothermal Amplification Buffer (New England Biolabs - NEB), 6 mM

MgSO4, 2 μM SYTO9 (ThermoFisher) and 8 U of Bst 2.0 DNA polymerase (New England Biolabs-NEB) or spores displaying Bst were added to the reaction.

The spore suspensions were normalized to an OD_{580nm} of 2 and diluted 1:2, 1:4, 1:8, 1:10 and 1:20 in reaction buffer. Spores were sedimented by centrifugation and resuspended in the reaction volume.

In case of RT-LAMP, the SARS-CoV-2 N-gene was amplified within a volume of 20 μL containing: 8 U Bst 2.0 (NEB), 2 μM SYTO (ThermoFisher), 1× master mix (1.6 μM SARS_FIP/BIP primers, 0.4 μM SARS_LF/LB primers, 0.2 μM SARS_F3/B3 primers Gene N-A [68]). 7.5 U RTx (NEB) or spores displaying FeLRT were added to the reaction. The spores suspension were normalized to an OD_{580nm} of 2 and diluted 1:5, 1:10 and 1:20 in reaction buffer. Spores were sedimented by centrifugation and resuspended in the reaction volume.

The reactions were performed at 65 ºC for 30 min with or without a pre-incubation at 42 ºC or 55 ºC for 5 min in a LightCycler480 or LightCycler 96 (Roche) thermocycler. Fluorescence was acquired every minute for 30 min.

2.3.7 RT-PCR enzyme assays

SARS-CoV-2 N-gene was amplified by RT-PCR using the KAPA SYBR FAST One-Step qRT-PCR Master Mix (Roche) and a LightCycler480 or LightCycler 96 (Roche) thermocycler, according to the manufacturer's instructions The reaction contained 1x KAPA SYBR Fast qPCR Master mix 2x and 200 nM of each primer N1-F and N1-R [69]. For testing the MashUp-RT display at the spore surface, spore suspensions were normalized to an OD_{580nm} of 2 and diluted 1:5, 1:10 and 1:20 in reaction buffer. Spores were sedimented by centrifugation and resuspended in the reaction volume.

2.4 Cell biology techniques

2.4.1 Fluorescence microscopy and image analysis

Spores, after measuring their OD_{580} on a suspension diluted in 1:200 in ddH_2O and applying the formula: μL/well: 3600/(OD_{580}*200), were fixed in 1 mL of HistoChoice Tissue Fixative MB (Amresco) at room temperature for 15 min, followed by 30 min in

ice. Then, the suspension was washed with 1 mL PBS-2% BSA three times and resuspended in 1 mL of the same solution. After an incubation of 30 min, the samples were centrifugated and the spores resuspended in 500 µL PBS-2% BSA with an anti-His_6Tag antibody (Novagen) diluted 1:500 and incubated overnight at 4 ºC. The following day, the spores were washed again in the same manner as above, resuspended in 500 µL PBS-2%BSA with Alexa Fluor 594 goat anti-mouse IgG diluted 1:250 (Molecular Probes) and incubated for 1 h at room temperature with agitation. After three more washes in PBS 1x, the spores were resuspended in 50 µL of PBS 1x, 3 µL were mounted onto glass slides coated with 1.7% agarose. The spores were observed on a Leica DM6000B microscope equipped with a phase contrast Uplan F1 100x objective. Images were acquired with a CCD Andor Ixon camera (Andor Technologies) and analysed using the Metamorph software suite (version 5.8; Universal Imaging). Figures were prepared using Adobe Photoshop and ImageJ/Fiji.

Chapter 3 – Results

3.1 Display of Bst at the spore surface

LAMP uses the large fragment of Bst DNA polymerase, from *Bacillus stearothermophillus,* for DNA amplification. The large fragment of this enzyme retains the 5'to 3' polymerase activity and thermal stability as the full-length protein, while it lacks the 5'to 3' exonuclease activity [70]. Bst also has strand displacement activity, which allows the polymerization reaction to occur at a constant temperature of 65 ºC. The display of this enzyme in a stable and secure platform would lower production and purification costs. As mentioned in the introduction, *B. subtilis* spores have been used with success as a display platform for enzymes [39, 70]. Even if the spore coat is permeable to small molecules, we considered that for our application it would be better to choose a protein from the crust, the outermost coat layer, as a carrier. Since CotZ and CotY are the two most abundant components of the crust we choose them as carrier proteins for Bst [72]. A *his$_6$ tag* was placed at the Bst N- and C-terminal fusions, which allows detection of the recombinant proteins using a commercial antibody with established specificity and efficacy, without the need for anti-Bst antibodies. A linker was also inserted in all protein fusions between the carrier protein and Bst. The linker used is composed of the EAAAK sequence that forms a short, rigid α-helix followed by the GGGS sequence, which assumes a flexible conformation [15, 73].

We used the SOE technique to construct a fusion of *cotZ-linker* to *bst-his$_6$.* Initially, the *cotZ-linker* and *bst* sequences were amplified separately, from chromosomal DNA obtained from a wild-type *B. subtilis* strain (PY79) and from pBST (which carries the *bst* gene; [57]), respectively. The following primer pairs were used (Annex 6.2): for *cotZ*, CotZ_Fw_HindIII and Bst_SOE_Lk_Rev_CotZ; and for *bst*, Bst_SOE_Lk_Fw_CotZ_Bst and Bst_His$_6$_Rev_BamHI. The 396 bp *cotZ-linker* fragment and the 1779 bp *bst* fragment were purified, mixed and amplified by slicing by overlay extension (SOE) with primers CotZ_Fw_HindIII and Bst_6XHis_Rev_BamHI (see above). This produced a 2175 bp *cotZ-linker-bst-his$_6$* fragment, which was cloned between the BamHI and HindIII restriction sites of plasmid pMS38 [74], yielding pCN01. This plasmid was used to transform strain PY79; a Cm^R transformant that was the result

of a single reciprocal crossover event (Campbell-type mechanism) was selected and designated MSB250 (Annex 6.1).

To create the *his$_6$-bst-linker-cotY* and *cotY-linker-bst-his$_6$* we used plasmids p1CSV-CotY-N and p1CSV-CotY-C [72], respectively, in which the fusion genes are under the control of the P_{cotZY} promoter, the strongest promoter from the *cotVWXYZ* operon (Fig. 2, [26]). These vectors also include the two halves of the non-essential *amyE* gene from *B. subtilis*, enabling integration at this locus by a double crossing-over that inactivates the gene and the identification of positive transformants by a simple starch test (see Materials and Methods). For *cotY-linker-bst- his$_6$*, the *bst* gene was amplified from pCN01 using the primers LK_Fw_AgeI and Bst_Rev_SpeI. The resulting 1851 bp fragment was inserted between the AgeI and SpeI sites of p1CSV-CotY-C, resulting in pCN02. To obtain the *his6-bst-linker-cotY* fragment, the *bst* gene (1779 bp) and linker (72 bp) were first amplified from pCN01 using the primer pairs Bst_Fw_XbaI and Lk_Rev_NgoMIV and Lk_SOE_Bst_Fw_Bst_CotY and NgoMIV_Lk_Rev, respectively. Both fragments were joined by SOE, resulting in an amplicon of 1851 bp, which was inserted between the XbaI and NgoMIV sites of plasmid p1CSV-CotY-N, yielding pCN03. pCN02 and pCN03 were used to transform strain PY79; Cm^R and $AmyE^-$ transformants were identified and designated MSB251 and MSB252, respectively (Annex 6.1).

Mutants for the genes coding for the crust proteins produce heat and lysozyme resistant spores, indicating that the use of the crust proteins as carriers should not affect the functional proprieties of the spores [75]. To test whether the assembly of Bst onto the spore crust would impact on the spore proprieties we start by testing heat and lysozyme resistance of the spores produced in DSM by the strains expressing CotZ-Bst-His_6, His_6-Bst-CotY or CotY-Bst-His_6 fusions (Fig 4; see Materials and Methods). As shown in figure 4A, spores from the strain carrying the CotZ-Bst-His_6 fusion has a behaviour similar to the wild type strain (without fusion protein, WT). In contrast, strains carrying the His_6-Bst-CotY and CotY-Bst-His_6 produce spores resistant to lysozyme but more sensitive to heat than the WT strain. Nevertheless, a titer of at least 10^8 spores/ml was attained in all the strains, which enables the efficient production and purification of spores for further testing. The crust proteins contribute to spore hydrophobicity, which in turn reduce the aggregation of the spores [20]. We used BATH assays to compare the relative

hydrophobicity of the recombinant spores with the WT (see Materials and Methods). As represented in figure 4B, spores purified from the strain producing CotZ-Bst-His_6 showed to be significantly more hydrophobic than the WT spores, while the spores purified from the strain producing the CotY fusions were more hydrophilic. These results indicate that the spore surface is altered in the recombinant strains.

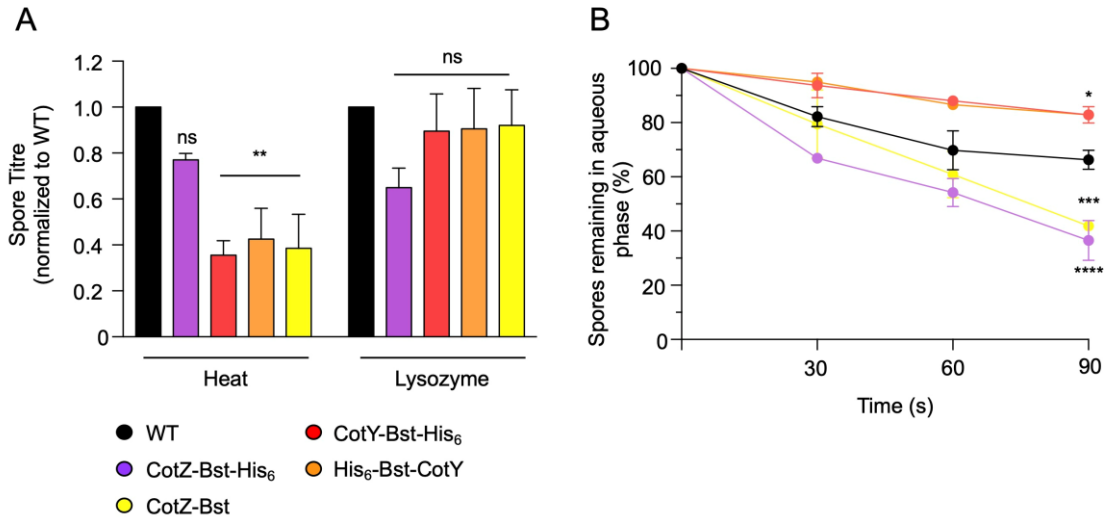

Figure 4. Bst fusion proteins modify the proprieties of spores. A) heat and lysozyme resistance tests, with the spore titre obtained for all the Bst-expressing strains normalized to the wild-type (WT). **B)** BATH assays conducted on all the Bst strains; measures were taken from the aqueous layer after mixing of the suspensions for four consecutive pulses of 0, 30, 60 and 90 sec each. The data represents the mean ± SD from 3 independent experiments. Asterisks indicate statistical significance determined by one-way ANOVA tests (ns, no significant; **** $p < 0.0001$; *** $p < 0.0001$; ** $p < 0.001$; * $p < 0.01$).

To test if the expression of the recombinant proteins had an impact on the protein composition of the spore surface layers, the spore coat and crust proteins were extracted from purified spores and resolved by SDS-PAGE. As shown in Fig. 5A, the spores of the strain producing the fusion protein His_6-Bst-CotY have a pattern of extractable proteins similar to the WT strain. We conclude that the fusion protein does not interfere in a major way with the normal assembly of the other proteins that form the spore coat and crust. In contrast, in the pattern of extractable proteins from spores carrying the CotZ-Bst-His_6 and CotY-Bst-His_6 fusion two bands of approximately 35 and 66 kDa appeared absent (Fig. 5A, red dots). Furthermore, an extra band, between the 75 and 100 kDa markers, is extracted from CotZ-Bst-His_6 spores, which may correspond to the fusion protein, which

has an expected size of 85 kDa (Fig. 5A, purple arrow). Bands that may correspond to His_6-Bst-CotY (87 kDa) and CotY-Bst-His_6 (87 kDa) were not detected in the SDS-PAGE of the coat/crust extracts stained with Coomassie (Fig 5A).

CotY is a cysteine rich protein that forms very stable multimeric complexes that are difficult to solubilize [25]. Thus, CotY is not easily identified in a normal SDS-PAGE stained with Coomassie and is usually detected using antibodies against the protein [76]. Here, we used an anti-His_6 to test for the presence of the fusion protein by immunoblot. As a negative control, we use the WT strain which does not carries a *his_6-tag* sequence. We monitored the accumulation of the fusion protein during sporulation in DSM, from hour 4 to 8 after the onset of sporulation, and its presence in coat/crust extracts obtained from purified spores. The His_6 antiserum detected the CotZ-Bst-His_6 (Fig. 5B; purple arrow) and His_6-Bst-CotY (Fig. 5B; orange arrow) fusion proteins during sporulation, mainly as a species of approximately 85 kDa; no species of this size was detected in the WT strain. In contrast, the CotY-Bst-His_6 fusion protein was not detected during sporulation; also, only the CotZ fusion was detected in purified spores (Fig. 5B; purple arrow).

Immunofluorescence microscopy using anti-His_6 antibody and anti-mouse-Alexa Fluor 594 was in agreement with the immunoblotting results (Fig. 5C). In CotZ-Bst-His_6 spores fluorescence signal was detected in 89% of the spores, forming a complete ring of fluorescence in 75% of the spores and a polar cap in 15% of the spores (Fig. 5C). This localization pattern is similar to the ones observed before using a CotZ-GFP fusion [27]. These results also show that CotZ-Bst-His_6 is produced and assembled at the surface of the spore, in a location that is accessible to the antibody. In contrast, the fusions CotY-Bst-His_6 and His_6-Bst-CotY were only detected in a lower fraction of the spores (21% and 3%, respectively) and always as a polar cap (Fig. 5C)

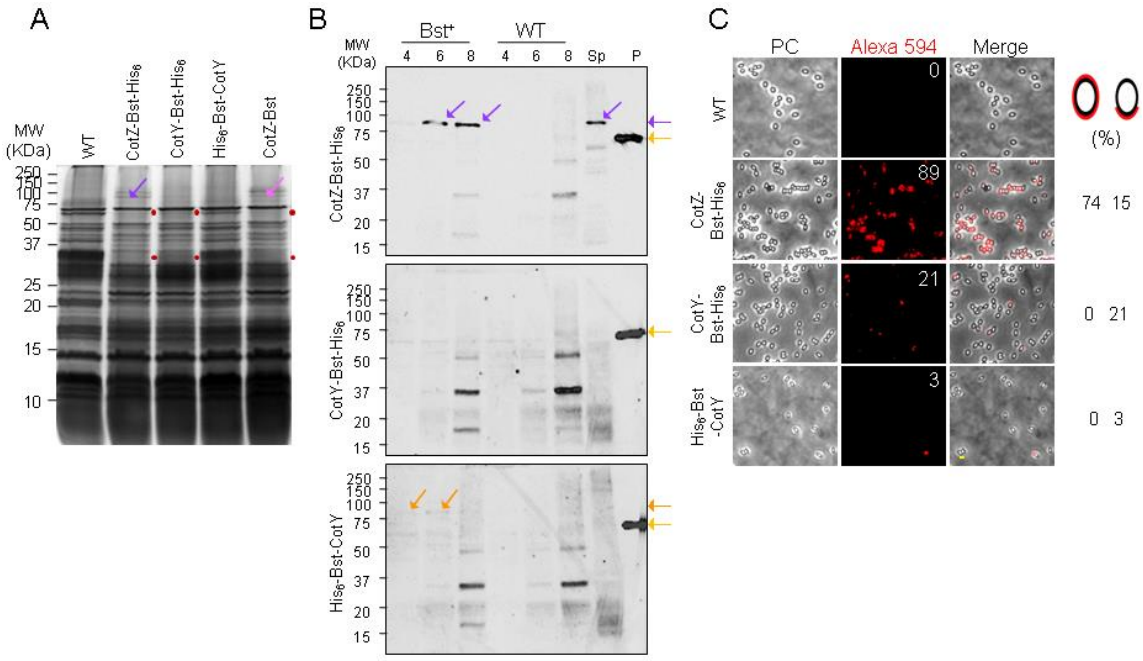

Figure 5. Display of Bst fusions at the spore crust. (A) SDS-DTT coat/crust protein extracts obtained from purified spores of the indicated strains. The extracted proteins were resolved on 15% polyacrylamide gels containing SDS (SDS-PAGE), and the gels stained with Coomassie blue. **(B)** detection of the fusion proteins by immunoblot analysis of coat/crust extracts and whole cell extracts of sporulating cells with an anti-His_6 antibody. Cell samples were collected from cultures at the represented times (in hours) after the onset of sporulation (T0). The yellow arrows show the position of purified Bst (67 kDa). The purple, pink and orange arrows show the position of CotZ-Bst-His_6, His_6-Bst-CotY and CotZ-Bst, respectively. **(C)** Imunofluorescence microscopy of the same strains using an anti-His_6 antibody and an anti-mouse secondary antibody coupled to Alexa 594. The percentage of cells emitting fluorescence signal were scored and separated in two classes according to the distribution of the fluorescens signal along the surface off the spore. Scale bar; 1µm

3.1.1 LAMP assays using recombinant spores

Since the best platform to display Bst was CotZ, we decided to start by testing recombinant spores carrying CotZ-Bst-His_6 for Bst activity using LAMP (Fig. 6, see Materials and Methods). LAMP reactions were performed with DNA from *Candida albicans*, using primers Ca_F3, Ca_B3, Ca_FIP, Ca_BIP and Ca_LB based on the ITS2 gene sequence [50]. Analysis of the amplification and melting curves of the LAMP reaction show amplification when the NEB Bst 2.0 was used (black curve, Fig 6A and C) but no amplification was detected when CotZ-Bst-His_6 spores, at different dilutions, were added to the reaction (green, red, blue and pink curves, Fig 6A and C). We considered the possibility that spores could absorb reaction components such as dNTPs, magnesium or the SYBR green, resulting in no amplification or detection of the genetic material. To test

if the spores would be inhibitory for the reaction, we added spores at different dilutions to the reaction with the NEB Bst 2.0. We found that the recombinant spores delay the reaction, but do not have an inhibitory effect that would explain the lack of activity observed when only spores were added to the reaction (Fig 6A and C, dashed lines).

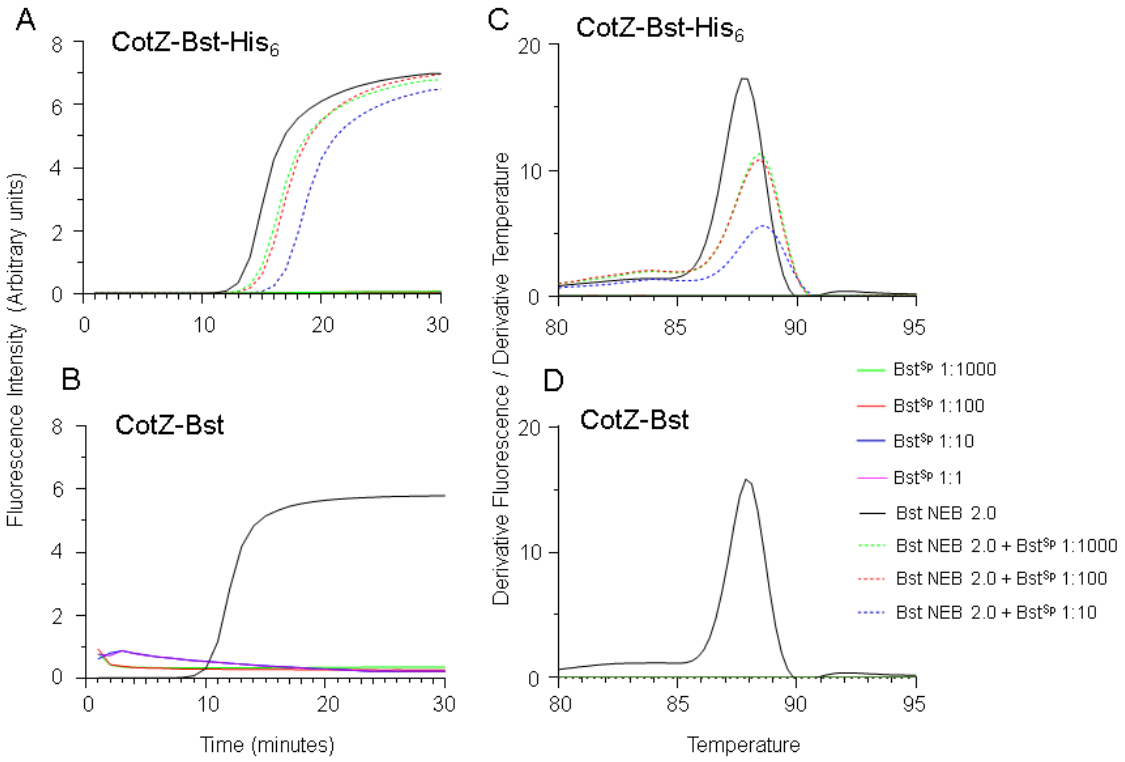

Figure 6. Spores displaying Bst fusions did not show DNA amplification activity. Amplification curves of the LAMP reaction using strains containing the fusions CotZ-Bst-His$_6$ **(A)** and CotZ-Bst **(B)**, tested at 4 different dilutions (1:1, 1:10, 1:100, 1:1000). Full lines represent the spores with their respective fusion in a reaction, while the dashed lines represent spores with their respective fusion mixed with the NEB Bst 2.0 enzyme. **C** and **D** show the respective melting curves of the reactions shown in **A** and **B**, respectively.

The results above suggest that the enzyme displayed at the surface of the spore is inactive. Inspection of the Bst structure (Annex 6.6) shows that the active site of the enzyme which includes residue of Asp^{540} is close to the C-terminal of the enzyme [70]. Since in the CotZ-Bst-His$_6$ fusion, a His$_6$ was added to the C-terminal of Bst, we hypothesized that this tag could interfere with the activity of the enzyme. For this reason, we constructed a new CotZ-Bst fusion, without the His$_6$-tag. For that purpose, plasmid pCN01 was submitted to Quickchange PCR, using the primer pair Quickchange_Fw and Quickchange_Rev to remove the His$_6$tag by adding a STOP codon just upstream the

respective coding sequence, yielding pCN06. This plasmid was transformed into strain PY79, and a Cm^R transformant was selected and designated MSB255(Annex 6.1).

Heat and lysozyme resistance test of spores produced in DSM by this strain show a similar behavior to the previous recombinant spores and hydrophobicity similar to the strain carrying the fusion CotZ-Bst-His_6 (Fig. 4A). Furthermore, the pattern of spore coat/crust proteins extracted from purified spores is similar to its counterpart carrying the His_6tag (Fig. 5A). Bands of 35 kDa and 66 kDa are missing from the pattern of extractable proteins from spores carrying the CotZ-Bst-His_6 and the CotZ-Bst fusion. An extra species is extracted from CotZ-Bst spores, between 75-100 kDa (Fig. 5A; pink arrow), which may correspond to the fusion protein, which has an expected size of 84.2 kDa. Due to the lack of a Bst antibody we were unable to detect this fusion in spores by immunoblot or fluorescence microscopy. The presence of the 85 kDa species, however, and the fact spore proprieties were similar to those of CotZ-Bst-His_6 bearing spores, suggests that this fusion is present in mature spores.

LAMP reactions were repeated as mentioned before, but now with different dilutions of spores produced by the strain carrying the CotZ-Bst fusion (Fig. 6B and D). Unfortunately, once again amplification was only detected when the commercial enzyme alone was used in the reaction (black curve, Fig 6B and D).

Spores carrying CotY-Bst-His_6 and His_6-Bst-CotY were also tested for Bst activity using LAMP, without success.

3.2 Display of MashUP-RT at the spore surface

Detection of RNA targets can be achieved by the addition of a reverse transcriptase (RT) to the LAMP reaction, this RT-LAMP is performed as a one-step isothermal amplification assay [68]. Taking into acount that RTs are usually more expensive and unstable than the Bst polymerase, this enzyme is also a very good candidate to display on the spore surface. In this study we used a modified version of the Feline Leukaemia Virus Reverse Transcriptase (FeLV-RT), the MashUp-RT. FeLV-RT is more accurate than the Moloney Murine Leukemia Virus Reverse Transcriptase (MMLV-RT), which is available commercially. The modified version MashUp-RT encoded in a plasmid kindly provided by Pipette Jockey [77], has its thermostability and accuracy increased by the removal of its RNase-H activity.

Like for Bst, we used CotZ and CotY as carrier to display the MashUp-RT to the spore surface, a *his$_6$ tag* was added at the *mashUp-RT* fusions and a linker was also inserted between the locus for the carrier protein and the gene coding for RT. To create the *cotZ-mashUp-RT-his$_6$* fusion we used genomic DNA from *B. subtilis* to PCR-amplify the *cotZ* gene (396 bp) using the primes CotZ_Fw_HindIII and SOE_FeLVRT_Rev_Z and the *mashUp-RT-his$_6$* (2022 bp) was amplified from pMashUp (Annex 6.3) using primers SOE_FeLVRT_Fw_Z and FeLVRT_Rev_Z. The two resulting DNA fragments were fused by SOE using CotZ_Fw_HindIII and FeLVRT_Rev_Z as the forward and reverse primers, respectively. The amplified product of 2418 bp was digested with BamHI and HindIII and inserted between the same sites of pMS38 [74] yield pCN05. This plasmid was transformed into PY79, a Cm^R transformant that was the result of a single reciprocal crossover event was identified and designated MSB254 (Annex 6.1). For *his$_6$-mashUp-RT-cotY*, first the *mashUp-RT* gene (2022 bp) was amplified from the plasmid pMashUp, using the primer pair XbaI_FeLVRT_FW and SOE_LK_FeLVRT_Rev, while the linker (72 bp) was amplified from pCN01 using the primers SOE_FeLVRT_Lk_Fw and NgoMIV_Lk_Rev. Both fragments were joined by SOE, resulting in a 2094 bp amplicon which was inserted between the XbaI and NgoMIV sites of the plasmid p1CSV-CotY-N, resulting in pCN04. pCN04 was used to transform the strain PY7; Cm^R and $AmyE^-$ transformant was identified and designated MSB253 (Annex 6.1).

Like in the Bst strains, the incorporation of the MashUp-RT in the crust could lead to changes in the resistance properties of the spore. We started by testing heat and lysozyme resistance (Fig. 7A). Expression of CotZ-MashUp-RT-His_6 and His_6-MashUp-RT-CotY fusion proteins did not change significantly the spores resistance to lysozyme. However, heat resistance was decreased in the recombinant spores. Once again, a titer of at least 10^8 spores/ml was attained in all the strains, which enables the efficient production and purification of spores for further testing. BATH assays show that purified spores from the strain producing CotZ-MashUp-RT-His_6 fusion behave like the WT strain, while the purified spores from the strain producing His_6-MashUp-RT-CotY fusions were more hydrophilic (Fig. 7B).

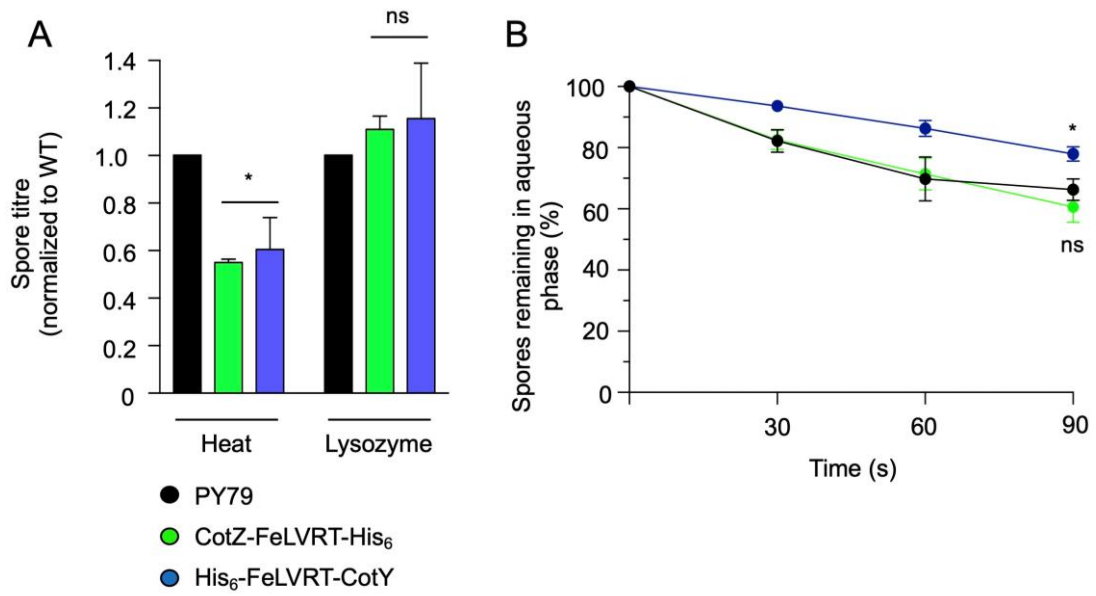

Figure 7. MashUp-RT fusion proteins modify the proprieties of spores. A) heat and lysozyme resistance tests, with the spore titer obtained for all MashUp-RT strains normalized to the wild-type (WT). **B)** BATH essays conducted on all the MashUp-RT strains. OD_{580} measurements were done of the aqueous layer after mixing of the suspension for four consecutive cycles of 0, 30, 60 and 90 sec. All data represent the means ± SD from 3 independent experiments. Asterisks indicate statistical significance determined by one-way ANOVA tests (ns, no significant; **** $p < 0.0001$; *** $p < 0.0001$; ** $p < 0.001$; * $p < 0.01$).

The pattern of coat/crust proteins extracted from the recombinant purified spores producing His_6-MashUp-RT-CotY are similar to the WT strain. Once again, in recombinant spores in which the CotZ protein is the carrier, the species at 35 and 66 kDa band are absent from the pattern of extractable proteins and an extra faint band, between the 75 and 100 kDa markers, is extracted (Fig. 8A; green arrow), that may correspond to the fusion protein (expected size of 93.1 kDa).

Immunoblot analysis with anti-His_6 antibody showed that both fusion proteins accumulate poorly during sporulation and are detected at low levels in mature spores (Fig. 8B, green arrow for CotZ-MashUp-RT-His_6 and blue arrow for His_6-MashUp-RT-CotY). Immunofluorescence microscopy using anti-His_6 antibody were in agreement with these results. Less than 50 % of the spores showed fluorescence (49 % for CotZ-MashUp-RT-His_6 and 9 % for His_6-MashUp-RT-CotY) and only a few of those showed a complete ring of fluorescence (16 % for CotZ-MashUp-RT-His_6 and 1 % for His_6-MashUp-RT-CotY; Fig. 8C).

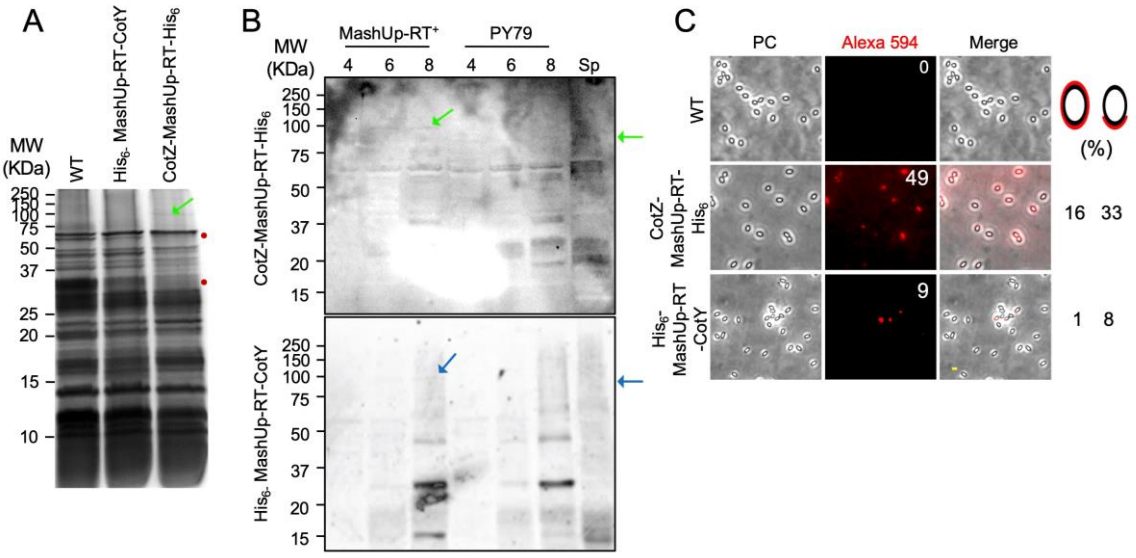

Figure 8. Display of MashUp-RT fusions at the spore crust. (A) SDS-DTT coat/crust protein extracts obtained from purified spores of the indicated strains. The extracted proteins were resolved on 15% polyacrylamide gels containing SDS, and the gels stained with Coomassie blue. **(B)** detection of fusion proteins by immunoblot analysis of coat/crust extracts and whole cell extracts of sporulating cells with an anti-His_6 antibody. Cell samples were collected from cultures at the represented times (in hours) after the onset of sporulation (T0). The green and blue arrows indicate the position of CotZ-MashUp-RT-His_6 and His_6-MashUp-RT-CotY, respectively. **(C)** Immunofluorescence microscopy of the same strains using an anti-His_6 antibody and an anti-mouse secondary antibody coupled to Alexa 594. The percentage of cells emitting a fluorescence signal were scored into two classes according to the surface coverage of the fluorescence signal. Scale bar; 1µm.

3.2.1 RT-LAMP assays using recombinant spores

To test the activity of the displayed MashUp-RT, spores of both strains were tested in RT-LAMP assays using RNA extracted from saliva of patients infected with SARS-CoV-2, as template for cDNA synthesis (Fig. 9). The primers GeneN-A-SARS_F3, SARS_B3, SARS_FIP, SARS_BIP, SARS_LF and SARS_LB based on the Gene N fragment sequence [68]. Figure 9A and 9B show the amplification curves for the RT-LAMP reaction with recombinant spores carrying CotZ-MashUp-RT-His_6 and His_6-MashUp-RT-CotY, respectively. The RT-LAMP reactions were done at 65 ºC. However, spore displayed proteins can have different requirements for their activity and other reverse transcriptases have their optimal activity ranging from 42 to 65 ºC. For this reason, we performed the RT-LAMP reaction with a two-step protocol, where the pre-incubation was done at three different temperatures, 42 ºC, 55 ºC and 65 ºC (Fig. 9). At all temperatures we detect amplification when the commercial enzymes Bst 2.0 and RTx

(NEB) or Bst 2.0 (NEB) alone were used (Fig. 9, black and red lines). The amplification with Bst alone can be explained by a basal RT activity of the NEB Bst 2.0 [41, 77]. At 42 ºC, this activity is enhanced in the presence of purified WT spores (Fig. 9, grey line compared with red line). At 42 ºC we were also able to detect amplification using the recombinant spores CotZ-MashUp-RT-His_6 and His_6-MashUp-RT-CotY. In case of the reaction, in which the dilution 1:10 of the His_6-MashUp-RT-CotY spores was added, the amplification occurs earlier than when WT spores were added (Fig. 9, blue lines compared with grey lines). We hypothesized that the earlier amplification detected is due to RT activity of the enzyme displayed at the spore surface.

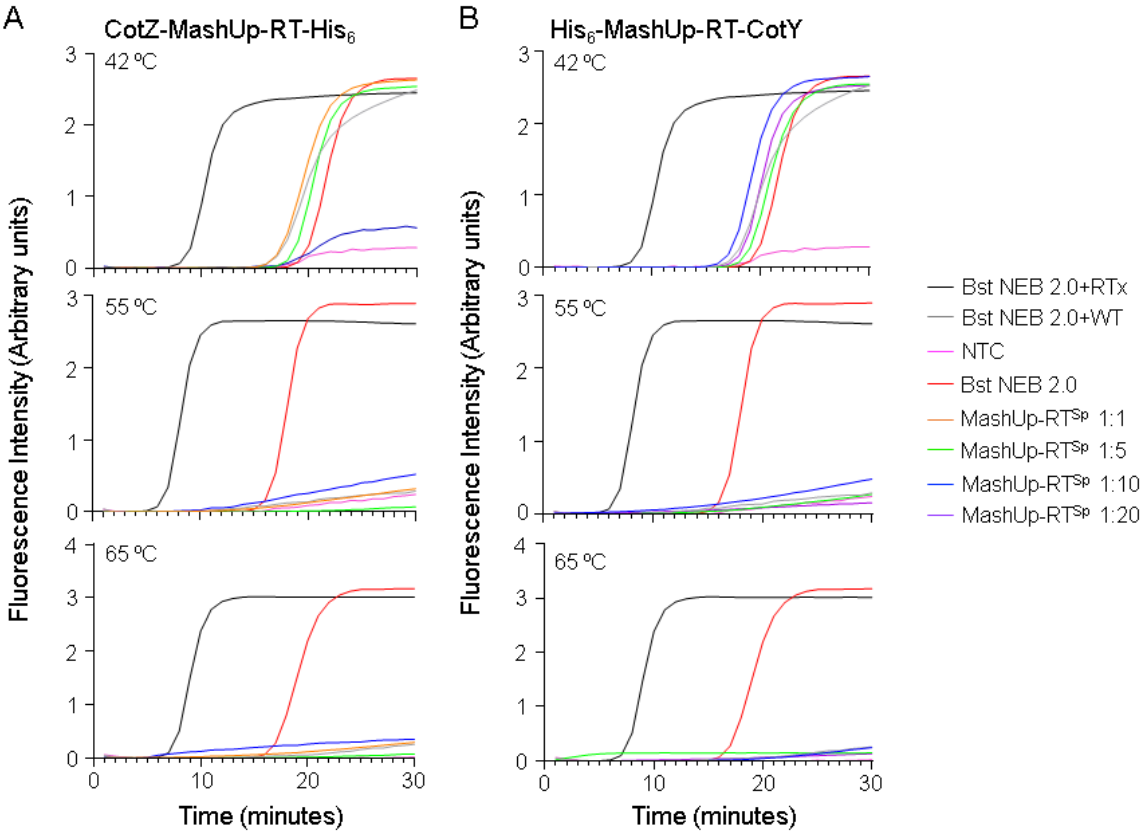

Figure 9. RT-LAMP assays using spores displaying CotZ-MashUp-RT-His_6 and His_6-MashUp-RT-CotY. Emitted fluorescence throughout 30 cycles in a RT-LAMP reaction using strains containing the fusions CotZ-MashUp-RT-His_6 **(A)** and His_6-MashUp-RT-CotY **(B)**, tested at four different dilutions (1:1, 1:5, 1:10, 1:20). All reactions were done at 65 ºC, and in the indicated reactions, preceded by a pre-incubation at 42 ºC or 55 ºC according to the range of temperatures in which the MashUp-RT was active.

As the basal Bst activity was interfering with conclusion that could be drawn in terms of RT activity, we tested whether the His_6-MashUp-RT-CotY spores, could replace the RT in RT-PCR assays (Fig. 10A).

RNA extracted from saliva of COVID-19 patients was used as template for cDNA synthetizes using primers N1-F and N1-R (see Materials and Methods). Analysis of the product of the reaction in agarose gel shows a band of 110 pb in the positive controls (reaction with commercial KAPA SYBR FAST One-Step RT-PCR). We also detected a faint band in the reaction in which a 1:10 dilution of recombinant spores carrying His_6-MashUp-RT-CotY was used. Analysis of the melting curves of these reactions showed cDNA synthesis at the 1:10 dilution (Fig. 10B, blue line) and 1:1 dilution (Fig. 10B, orange line) and show that the cDNA synthetized is specific, since it has the same melting temperature then the positive controls.

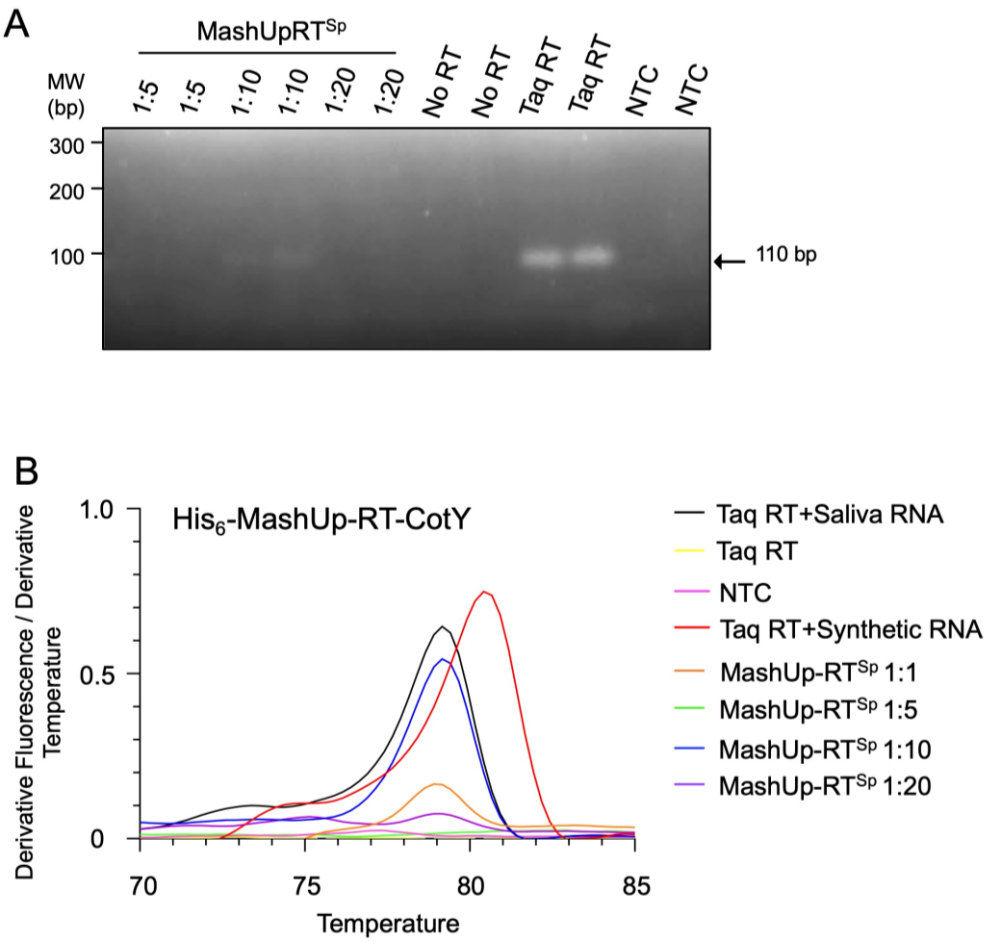

Figure 10. RT-PCR using spores displaying His6-MashUp-CotY. A) 2% agarose gel with the product of the RT-PCR reactions. cDNA synthesis of 110 bp of the N-gene from SARS-CoV-2 was performed. All spores dilutions and controls were done in duplicates. The molecular weight (MW) marker is indicated in base pairs (bp) on the left side. B) Melting curves of the RT-PCR reaction using purified spores from strains producing His6-MashUp-RT-CotY. Four different spore dilutions (1:1, 1:5, 1:10, 1:20) were tested. Two positive controls were done using viral RNA (black lines) and synthetic RNA (red lines) with the commercial Taq RT. The negative control for the RT (yellow lines) had no RNA in the reaction mix, and the negative control for the RNA (pink lines) had a non-template RNA.

Chapter 4 – Discussion and Conclusion

One of the major challenges in nanotechnology is the discovery of platforms for the display of useful biomolecules. These platforms have to be highly stable, easy to produce, easy to manipulate and with a large useable surface area. Spores from *Bacillus subtilis* meet all these criteria. Spores can withstand harsh environments such as desiccation, heat, solvents, lytic enzymes, oxidizing agents, ultraviolet radiation, and predators [12]. Spores are easy to produce and can be stored at room temperature for long periods of time [79]. Moreover, *B. subtilis* is genetically manipulated with ease and is also recognised as a safe organism, with GRAS status [80]. Because of all these characteristics, spore surface display has already been successfully applied to fields such as oral vaccines [81], biopesticides [82], bioremediation [83] and animal feed [39].

During the COVID-19 pandemic, high demand for SARS-CoV-2 testing and disruption of global supply chains have left many countries facing diagnostic shortages. A proposed solution for these problems was the local production of affordable diagnostic tests [55, 67, 83]. In previous work, a RT-LAMP test for SARS-CoV-2 detection in RNA samples extracted from the saliva of COVID-19 patients was established [57]. RT-LAMP-based tests have gained popularity due to their advantages over those based on RT-PCR [46, 84]. The enzymes used in the implementation of a SARS-CoV-2 diagnostic LAMP-based test by Amaral and colleagues (Bst and MashUp-RT) were all in-house-made, making the test independent of commercial reagents [57], however still dependent of the production and multi-step purification methodologies which requires specific equipment.

To our knowledge, spore display of enzymes for molecular diagnosis has never been reported. The use of such a strategy, however, would facilitate production of the enzymes, bypassing the purification steps, with the concomitant decrease in production costs. In this work we used the crust proteins CotZ and CotY as carrier/anchoring proteins to display the DNA polymerase Bst and the reverse transcriptase MashUp-RT at the spore surface, for molecular diagnosis using RT-LAMP. The CotZ and CotY proteins have already been used to successfully display active ß-galactosidase and laccase at the spore surface [85, 86]

Immunoblot and immunofluorescence experiments showed that CotZ-Bst-His_6 was displayed at the spore surface (Fig.5). In contrast, when CotY was used as the carrier protein, the fusion protein was only detected in a low percentage of the spores (Fig. 5). The *cotY*-based fusions were inserted at the *amyE* locus, keeping the native *cotY* gene in the chromosome. The preferential assembly of the native CotY may explain the low percentage of spores showing fluorescence signal, *i.e.*, the fusion competing poorly with the WT CotY for a limited number of assembly sites. It is also possible that the CotY fusion shows a more internal localization, not accessible to the antibody, or the protein is highly cross-linked, and is not efficiently extracted in our conditions. We do not favour these hypotheses since we also did not detect the fusion proteins during sporulation, at a time when the spore is not yet formed and the proteins are more extractable (Fig. 5B). Presumably, then, the fusion proteins are unstable and accumulate to low levels in sporulating cells.

CotZ-Bst spores were resistant to heat and lysozyme but more hydrophobic than the WT spores, indicating that the spore surface was perturbed (Fig. 4). A high level of hydrophobicity is not desirable since it interferes with the adherence to surfaces and promote clumping of spores, decreasing the surface exposed to the environment and potentially having a negative impact in the LAMP and RT-LAMP assays [20]. Assembly of CotZ-Bst-His_6 (and also CotZ-Bst) strongly reduced the representation of a 34 and a 66 kDa species extracted from WT spores by boiling in the presence of SDS-DTT (Fig. 5A). These two proteins are likely to be CotG and CotB [74]. Previous studies have shown that the absence of the crust, namely the absence of the proteins CotX, CotY and CotZ, have an impact on the outer coat [27]. Therefore, the crust proteins have a role in the localization of the outer coat proteins, including CotG and CotB. CotB is synthesized as a 46 kDa protein and is converted into a 66 kDa form by phosphorylation. Both CotB and CotG are phosphorylated by CotH and CotG is required for the efficient phosphorylation of CotB [27, 73, 87]. Therefore, in the absence of CotH and CotG, the CotB form of 66 kDa does not accumulate in the spore [74]. Western blot analysis using CotH, CotB and CotG antibodies would enable to identify at which stage our fusion protein (CotZ-Bst-His_6) impacts on the assembly of the spore outer coat.

Unfortunately, we were not able to detect any DNA amplification in the spores displaying Bst. A quantitative analysis of the amount CotZ-Bst-His_6 protein present at the

spore surface showed that when spores were normalized to an OD_{580nm} of 2, the amount of Bst in the spore was similar to the amount of NEB Bst 2.0 enzyme used in the reaction (approximately 4 ng/μl). In the future, it would be worth to test different reaction conditions, such as different temperature and pH values. The reaction conditions used in this work were optimized for the purified Bst, but its fusion to the carrier protein may have changed the enzyme´s kinetic properties. Also, optimization of the coat protein used for displayed or the protein linker sequences could be investigated in the future. Another carrier protein that could be used is CotG, one of the most abundant coat proteins, shown to localize together with CotW and CotZ in the outermost surface of the coat [89]. We could also use a longer linker, for example four repeats of the EAAAK sequence which forms a 20-Å-long rigid α-helix; in the past, the use of such a linker ensured functionality of a Tgl-CFP fusion [15].

A new method based on the SpyTag-SpyCatcher technology could also be adapted to display Bst at the spore surface. This system is formed by two proteins: the larger SpyCatcher that can bind specifically to the smaller, SpyTag, forming an intermolecular spontaneous isopeptide bond between the two [90]. The Bst protein would be fused to the SpyTag since it is the smaller unit and thus should interfere less with the folding and/or activity of the enzyme, while the SpyCatcher would be fused to CotZ or CotY, allowing the anchoring of the target protein once the bond is formed (Fig. 11). Cells of *B. subtilis* would express the Bst-SpyTag at a late time during sporulation, after the production and assembly of the carrier-SpyTag to minimize problems with the assembly of the fusion protein. The Spy/Catcher system has been used for visualising membrane protein location, vaccine efficiency and others; we think it may be a good alternative method for displaying proteins at the spore surface [88, 89].

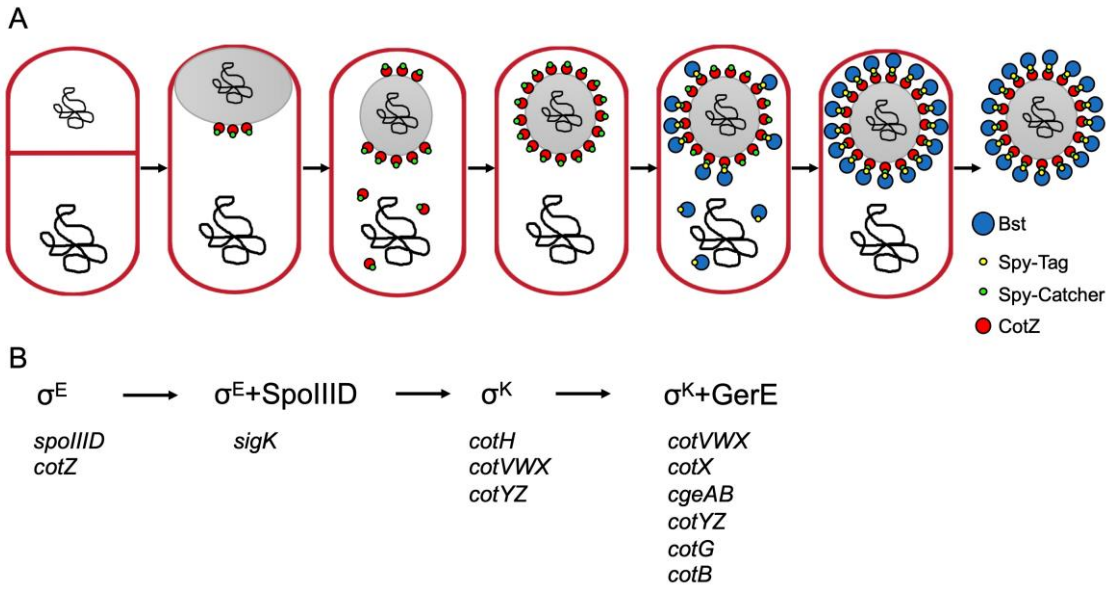

Figure 11. Scheme of the spore surface display using SpyTag-SpyCatcher. A) After asymmetric division, σ^E is activated in the mother cell and the transcriptional and translation signals of *cotZ* allows expression of the CotZ-Spy-Catcher fusion protein in the mother cell. The fusion protein is assembled around the forespore, forming a complete ring after engulfment, concomitant with σ^K activation. Bst-Spy-tag is expressed late during sporulation under the regulation of a σ^E and GerE dependent promotor, such as *cgeAB*. Spontaneous isopeptide bond formation occurs through reaction of Lys31 of SpyCatcher with Asp117 of SpyTag, wich will anchor Bst to the spore surface. At the end of the sporulation process, the mother cell lyses and the spore displaying Bst is release to the environment. **B)** Simplified scheme of the mother cell cascade of gene expression. Examples of genes under the control of σ^E, SpoIIID, σ^K and GerE are given. Adapted from [15].

In the case of the MashUp-RT, two different strains were constructed. Phenotypically, these strains behave in a similar way as their counterparts carrying Bst (Fig. 7). However, in both MashUp-RT-producing strains only a small percentage of the spores displayed the fusion protein at the surface (Fig. 8). In any case, a clear RT enzymatic activity was demonstrated for spores carrying His_6- MashUp-RT -CotY (Fig. 9 and 10). This activity, however, was only detected when a pre-incubation of 42 ºC was implemented, which is not the optimal temperature for RT-LAMP (65 ºC). In agreement with previous studies [91, 92], in our assays the commercial Bst showed RT activity [78]. Surprisingly, the presence of WT spores seems to enhance this activity (Fig. 9). These results suggest that the spore is able to stabilize the reverse transcriptase activity of different enzymes, even when WT spores are added to the free enzyme, *i.e.*, not surface displayed.

In conclusion, we were able to display the enzymes Bst and MashUp-RT at the spore surface. Unfortunately, only MashUp-RT showed activity. We used two different anchoring proteins, with N- and C-terminal variants. As illustrated by our own results, the display of proteins in spores is not a "one size fits all" methodology, the efficiency of this technology will always depend on the individual combination of the proteins used. In any case, this technology still represents a more economical way to produce, purify and stabilize enzymes, and for that, we think it is worth to continue the optimization of this strategy in order to obtain spores displaying active MashUp-RT and Bst enzymes to be used in RT-LAMP. An ultimate goal would be to construct strain that produce a high titer of spores and display both enzymes at the surface of the same spore, which could minimize diffusion distances between substrates and enzymes increasing reaction rates (Fig. 12).

Although the COVID-19 pandemic was the initial motivation for this work, in the longer term this technology can be used for the molecular diagnostic of other pathogens, which would certainly be an asset for public health in developed and developing countries.

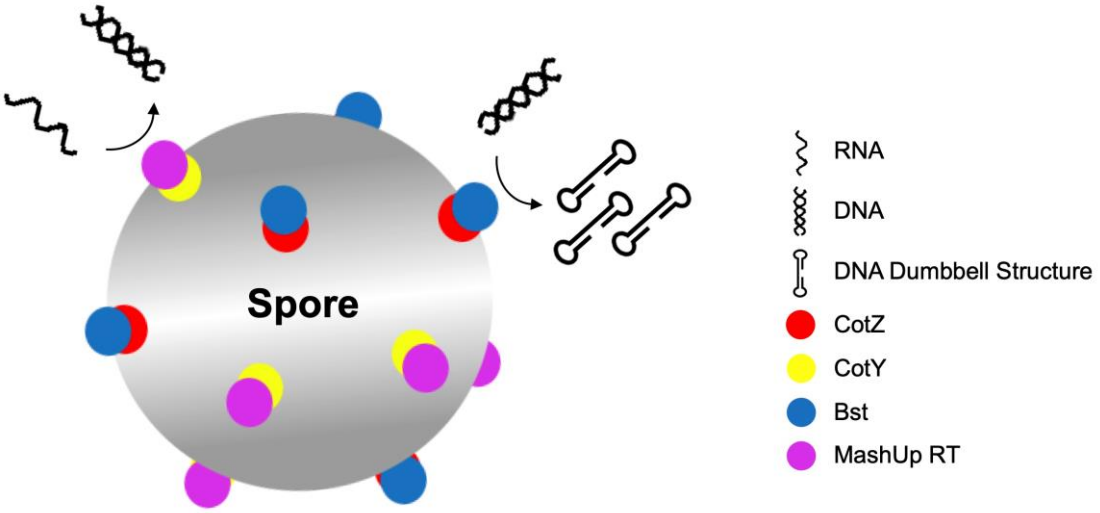

Figure 12. Spore display for RT-LAMP. Two crust proteins from *Bacillus subtilis* Spores, the CotZ and CotY, would be used as anchor proteins for the RT-LAMP enzymes, the Bst and the Mashup-RT, resulting on their display in the spores surface. When added to the reaction, the Mashup-RT would convert the RNA molecules to cDNA, which would be amplified by the Bst, resulting in the dumbbell structures.

Chapter 5 – References

[1] R. Ichhpujani, *Essentials of Medical Microbiology*. Jaypee Brothers Medical Publishers (P) Ltd., 2008.

[2] Y. Su, C. Liu, H. Fang, and D. Zhang, "Bacillus subtilis: a universal cell factory for industry, agriculture, biomaterials and medicine," *Microb. Cell Fact.*, vol. 19, no. 1, p. 173, Dec. 2020, doi: 10.1186/s12934-020-01436-8.

[3] H. A. Hong *et al.*, "Bacillus subtilis isolated from the human gastrointestinal tract.," *Res. Microbiol.*, vol. 160, no. 2, pp. 134–43, Mar. 2009, doi: 10.1016/j.resmic.2008.11.002.

[4] G. Drews, "The roots of microbiology and the influence of Ferdinand Cohn on microbiology of the 19th century," *FEMS Microbiol. Rev.*, vol. 24, no. 3, pp. 225–249, Jul. 2000, doi: 10.1111/j.1574-6976.2000.tb00540.x.

[5] F. Kunst *et al.*, "The complete genome sequence of the Gram-positive bacterium Bacillus subtilis," *Nature*, vol. 390, no. 6657, pp. 249–256, Nov. 1997, doi: 10.1038/36786.

[6] J. Errington and L. T. van der Aart, "Microbe Profile: Bacillus subtilis: model organism for cellular development, and industrial workhorse.," *Microbiology*, vol. 166, no. 5, pp. 425–427, 2020, doi: 10.1099/mic.0.000922.

[7] E. J, "Regulation of endospore formation in Bacillus subtilis," *Nat. Rev. Microbiol.*, vol. 1, no. 2, 2003, doi: 10.1038/NRMICRO750.

[8] M. PT, D. A, and E. P, "The Bacillus subtilis endospore: assembly and functions of the multilayered coat," *Nat. Rev. Microbiol.*, vol. 11, no. 1, 2013, doi: 10.1038/NRMICRO2921.

[9] M. Basta and P. Annamaraju, "Bacterial Spores," Feb. 2022, Accessed: Oct. 08, 2022. [Online]. Available: https://www.ncbi.nlm.nih.gov/books/NBK556071/.

[10] P. Eichenberger *et al.*, "The program of gene transcription for a single differentiating cell type during sporulation in Bacillus subtilis.," *PLoS Biol.*, vol. 2, no. 10, p. e328, Oct. 2004, doi: 10.1371/journal.pbio.0020328.

[11] J. Narula, A. Kuchina, F. Zhang, M. Fujita, G. M. Süel, and O. A. Igoshin, "Slowdown of growth controls cellular differentiation.," *Mol. Syst. Biol.*, vol. 12, no. 5, p. 871, 2016, doi: 10.15252/msb.20156691.

[12] A. O. Henriques and C. P. Moran, “Structure, assembly, and function of the spore surface layers.,” *Annu. Rev. Microbiol.*, vol. 61, pp. 555–88, 2007, doi: 10.1146/annurev.micro.61.080706.093224.

[13] S. T. Wang *et al.*, “The forespore line of gene expression in Bacillus subtilis.,” *J. Mol. Biol.*, vol. 358, no. 1, pp. 16–37, Apr. 2006, doi: 10.1016/j.jmb.2006.01.059.

[14] F. Nunes *et al.*, “SpoVID functions as a non-competitive hub that connects the modules for assembly of the inner and outer spore coat layers in Bacillus subtilis,” *Mol. Microbiol.*, vol. 110, no. 4, p. 576, 2018, doi: 10.1111/MMI.14116.

[15] C. G. Fernandes *et al.*, “Temporal and spatial regulation of protein cross-linking by the pre-assembled substrates of a Bacillus subtilis spore coat transglutaminase.,” *PLoS Genet.*, vol. 15, no. 4, p. e1007912, 2019, doi: 10.1371/journal.pgen.1007912.

[16] R. T. Eijlander, S. Holsappel, A. de Jong, A. Ghosh, G. Christie, and O. P. Kuipers, “SpoVT: From Fine-Tuning Regulator in Bacillus subtilis to Essential Sporulation Protein in Bacillus cereus.,” *Front. Microbiol.*, vol. 7, p. 1607, 2016, doi: 10.3389/fmicb.2016.01607.

[17] P. J. Piggot and D. W. Hilbert, “Sporulation of Bacillus subtilis.,” *Curr. Opin. Microbiol.*, vol. 7, no. 6, pp. 579–86, Dec. 2004, doi: 10.1016/j.mib.2004.10.001.

[18] S. Cutting, V. Oke, A. Driks, R. Losick, S. Lu, and L. Kroos, “A forespore checkpoint for mother cell gene expression during development in B. subtilis,” *Cell*, vol. 62, no. 2, pp. 239–250, Jul. 1990, doi: 10.1016/0092-8674(90)90362-I.

[19] G. W. Gould, “History of science - Spores: Lewis B Perry Memorial Lecture 2005,” *J. Appl. Microbiol.*, vol. 101, no. 3, pp. 507–513, 2006, doi: 10.1111/j.1365-2672.2006.02888.x.

[20] B. Shuster *et al.*, “Contributions of crust proteins to spore surface properties in Bacillus subtilis.,” *Mol. Microbiol.*, vol. 111, no. 3, pp. 825–843, 2019, doi: 10.1111/mmi.14194.

[21] S. GC, “The Exosporium Layer of Bacterial Spores: a Connection to the Environment and the Infected Host,” *Microbiol. Mol. Biol. Rev.*, vol. 79, no. 4, 2015, doi: 10.1128/MMBR.00050-15.

[22] D. Krajčíková, V. Bugárová, and I. Barák, “Interactions of Bacillus subtilis Basement Spore Coat Layer Proteins,” *Microorganisms*, vol. 9, no. 2, p. 285, Jan. 2021, doi: 10.3390/microorganisms9020285.

[23] E. Y. Kim, E. R. Tyndall, K. C. Huang, F. Tian, and K. S. Ramamurthi, “Dash-and-Recruit Mechanism Drives Membrane Curvature Recognition by the Small Bacterial Protein SpoVM.,” *Cell Syst.*, vol. 5, no. 5, pp. 518-526.e3, Nov. 2017, doi: 10.1016/j.cels.2017.10.004.

[24] P. T. McKenney and P. Eichenberger, “Dynamics of spore coat morphogenesis in Bacillus subtilis,” *Mol. Microbiol.*, vol. 83, no. 2, pp. 245–260, 2012, doi: 10.1111/j.1365-2958.2011.07936.x.

[25] Z. J, I. H, H. R, K. L, and A. AI, “Regulation of the transcription of a cluster of Bacillus subtilis spore coat genes,” *J. Mol. Biol.*, vol. 240, no. 5, 1994, doi: 10.1006/JMBI.1994.1456.

[26] J. Bartels, A. Blüher, S. López Castellanos, M. Richter, M. Günther, and T. Mascher, “The Bacillus subtilis endospore crust: protein interaction network, architecture and glycosylation state of a potential glycoprotein layer,” *Mol. Microbiol.*, vol. 112, no. 5, pp. 1576–1592, 2019, doi: 10.1111/mmi.14381.

[27] C. Freitas *et al.*, “RESEARCH ARTICLE A protein phosphorylation module patterns the Bacillus subtilis spore outer coat,” no. June, pp. 934–951, 2020, doi: 10.1111/mmi.14562.

[28] S. Jiang *et al.*, “Diverse supramolecular structures formed by self-assembling proteins of the Bacillus subtilis spore coat.,” *Mol. Microbiol.*, vol. 97, no. 2, pp. 347–59, Jul. 2015, doi: 10.1111/mmi.13030.

[29] G. M. Cherf and J. R. Cochran, “Applications of Yeast Surface Display for Protein Engineering.,” *Methods Mol. Biol.*, vol. 1319, pp. 155–75, 2015, doi: 10.1007/978-1-4939-2748-7_8.

[30] R. Isticato and E. Ricca, “Spore Surface Display,” *Microbiol. Spectr.*, vol. 2, no. 5, 2014, doi: 10.1128/microbiolspec.tbs-0011-2012.

[31] T. Anand *et al.*, “Phage Display Technique as a Tool for Diagnosis and Antibody Selection for Coronaviruses.,” *Curr. Microbiol.*, vol. 78, no. 4, pp. 1124–1134, Apr. 2021, doi: 10.1007/s00284-021-02398-9.

[32] S. Shave, S. Mann, J. Koszela, A. Kerr, and M. Auer, “PuLSE: Quality control and quantification of peptide sequences explored by phage display libraries,” *PLoS One*, vol. 13, no. 2, p. e0193332, Feb. 2018, doi: 10.1371/journal.pone.0193332.

[33] R. Rajput, M. Khanna, and H. K. Pradhan, “Phage-display technology for the production

of recombinant monoclonal antibodies," *Mater. Methods*, vol. 4, no. June, 2014, doi: 10.13070/mm.en.4.873.

[34] S. Y. Lee, J. H. Choi, and Z. Xu, "Microbial cell-surface display.," *Trends Biotechnol.*, vol. 21, no. 1, pp. 45–52, Jan. 2003, doi: 10.1016/s0167-7799(02)00006-9.

[35] R. E, B. L, and I. R, "Spore-adsorption: Mechanism and applications of a non-recombinant display system," *Biotechnol. Adv.*, vol. 47, 2021, doi: 10.1016/J.BIOTECHADV.2020.107693.

[36] S. T, S. A, I. R, D. F. M, M. M, and R. E, "Adsorption of β-galactosidase of Alicyclobacillus acidocaldarius on wild type and mutants spores of Bacillus subtilis," *Microb. Cell Fact.*, vol. 11, 2012, doi: 10.1186/1475-2859-11-100.

[37] R. Isticato *et al.*, "Non-recombinant display of the B subunit of the heat labile toxin of Escherichia coli on wild type and mutant spores of Bacillus subtilis," *Microb. Cell Fact.*, vol. 12, no. 1, p. 98, Dec. 2013, doi: 10.1186/1475-2859-12-98.

[38] J.-G. Pan, S.-K. Choi, H.-C. Jung, and E.-J. Kim, "Display of native proteins on *Bacillus subtilis* spores," *FEMS Microbiol. Lett.*, vol. 358, no. 2, pp. 209–217, Sep. 2014, doi: 10.1111/1574-6968.12558.

[39] S. Potot, C. R. Serra, A. O. Henriques, and G. Schyns, "Display of recombinant proteins on Bacillus subtilis spores, using a coat-associated enzyme as the carrier," *Appl. Environ. Microbiol.*, vol. 76, no. 17, pp. 5926–5933, 2010, doi: 10.1128/AEM.01103-10.

[40] R. Isticato *et al.*, "Surface display of recombinant proteins on Bacillus subtilis spores.," *J. Bacteriol.*, vol. 183, no. 21, pp. 6294–301, Nov. 2001, doi: 10.1128/JB.183.21.6294-6301.2001.

[41] H. Wang, Y. Wang, and R. Yang, "Recent progress in Bacillus subtilis spore-surface display: concept, progress, and future.," *Appl. Microbiol. Biotechnol.*, vol. 101, no. 3, pp. 933–949, Feb. 2017, doi: 10.1007/s00253-016-8080-9.

[42] P. Lin, H. Yuan, J. Du, K. Liu, H. Liu, and T. Wang, "Progress in research and application development of surface display technology using Bacillus subtilis spores," *Appl. Microbiol. Biotechnol.*, vol. 104, no. 6, pp. 2319–2331, Mar. 2020, doi: 10.1007/s00253-020-10348-x.

[43] L. Chen, A. Mulchandani, and X. Ge, "Spore-displayed enzyme cascade with tunable stoichiometry.," *Biotechnol. Prog.*, vol. 33, no. 2, pp. 383–389, 2017, doi:

10.1002/btpr.2416.

[44] S. Dwivedi *et al.*, “Diseases and Molecular Diagnostics: A Step Closer to Precision Medicine.,” *Indian J. Clin. Biochem.*, vol. 32, no. 4, pp. 374–398, Oct. 2017, doi: 10.1007/s12291-017-0688-8.

[45] P. Rai, B. K. Kumar, V. K. Deekshit, I. Karunasagar, and I. Karunasagar, “Detection technologies and recent developments in the diagnosis of COVID-19 infection,” *Appl. Microbiol. Biotechnol.*, vol. 105, no. 2, pp. 441–455, 2021, doi: 10.1007/s00253-020-11061-5.

[46] I. M *et al.*, “Diagnostic accuracy of LAMP versus PCR over the course of SARS-CoV-2 infection,” *Int. J. Infect. Dis.*, vol. 107, 2021, doi: 10.1016/J.IJID.2021.04.018.

[47] N. Tomita, Y. Mori, H. Kanda, and T. Notomi, “Loop-mediated isothermal amplification (LAMP) of gene sequences and simple visual detection of products,” *Nat. Protoc.*, vol. 3, no. 5, pp. 877–882, May 2008, doi: 10.1038/nprot.2008.57.

[48] B. de Oliveira Coelho *et al.*, “Essential properties and pitfalls of colorimetric Reverse Transcription Loop-mediated Isothermal Amplification as a point-of-care test for SARS-CoV-2 diagnosis,” *Mol. Med.*, vol. 27, no. 1, 2021, doi: 10.1186/s10020-021-00289-0.

[49] R. Lu *et al.*, “Development of a Novel Reverse Transcription Loop-Mediated Isothermal Amplification Method for Rapid Detection of SARS-CoV-2,” *Virol. Sin.*, vol. 35, no. 3, pp. 344–347, 2020, doi: 10.1007/s12250-020-00218-1.

[50] S. Fallahi, M. Babaei, A. Rostami, H. Mirahmadi, Z. Arab-Mazar, and A. Sepahvand, “Diagnosis of Candida albicans: conventional diagnostic methods compared to the loop-mediated isothermal amplification (LAMP) assay,” *Arch. Microbiol.*, vol. 202, no. 2, pp. 275–282, 2020, doi: 10.1007/s00203-019-01736-7.

[51] N. Ben-Assa *et al.*, “Direct on-the-spot detection of SARS-CoV-2 in patients,” *Exp. Biol. Med.*, vol. 245, no. 14, pp. 1187–1193, 2020, doi: 10.1177/1535370220941819.

[52] T. L. Quyen, T. A. Ngo, D. D. Bang, M. Madsen, and A. Wolff, “Classification of Multiple DNA Dyes Based on Inhibition Effects on Real-Time Loop-Mediated Isothermal Amplification (LAMP): Prospect for Point of Care Setting,” *Front. Microbiol.*, vol. 10, p. 2234, Oct. 2019, doi: 10.3389/fmicb.2019.02234.

[53] J. Fischbach, N. C. Xander, M. Frohme, and J. F. Glökler, “Shining a light on LAMP assays’ A comparison of LAMP visualization methods including the novel use of

berberine," *Biotechniques*, vol. 58, no. 4, pp. 189–194, Apr. 2015, doi: 10.2144/000114275.

[54] N. A. Tanner, Y. Zhang, and T. C. Evans, "Visual detection of isothermal nucleic acid amplification using pH-sensitive dyes," *Biotechniques*, vol. 58, no. 2, pp. 59–68, Feb. 2015, doi: 10.2144/000114253.

[55] L. E. Lamb, S. N. Bartolone, E. Ward, and M. B. Chancellor, "Rapid detection of novel coronavirus/Severe Acute Respiratory Syndrome Coronavirus 2 (SARS-CoV-2) by reverse transcription-loop-mediated isothermal amplification," *PLoS One*, vol. 15, no. 6, p. e0234682, Jun. 2020, doi: 10.1371/journal.pone.0234682.

[56] L. Mautner *et al.*, "Rapid point-of-care detection of SARS-CoV-2 using reverse transcription loop-mediated isothermal amplification (RT-LAMP)," *Virol. J.*, vol. 17, no. 1, pp. 1–14, 2020, doi: 10.1186/s12985-020-01435-6.

[57] C. Amaral *et al.*, "A molecular test based on RT-LAMP for rapid, sensitive and inexpensive colorimetric detection of SARS-CoV-2 in clinical samples," *Scientific Reports*, vol. 11, no. 1. 2021, doi: 10.1038/s41598-021-95799-6.

[58] L. Becherer *et al.*, "Point-of-Care System for HTLV-1 Proviral Load Quantification by Digital Mediator Displacement LAMP.," *Micromachines*, vol. 12, no. 2, Feb. 2021, doi: 10.3390/mi12020159.

[59] C. O. Nzelu, H. Kato, and N. C. Peters, "Loop-mediated isothermal amplification (LAMP): An advanced molecular point-of-care technique for the detection of Leishmania infection.," *PLoS Negl. Trop. Dis.*, vol. 13, no. 11, p. e0007698, 2019, doi: 10.1371/journal.pntd.0007698.

[60] M. Saar, M. Beissner, F. Gültekin, I. Maman, K.-H. Herbinger, and G. Bretzel, "RLEP LAMP for the laboratory confirmation of leprosy: towards a point-of-care test.," *BMC Infect. Dis.*, vol. 21, no. 1, p. 1186, Nov. 2021, doi: 10.1186/s12879-021-06882-2.

[61] T. Song, F. Wang, S. Xiong, and H. Jiang, "Surface display of organophosphorus-degrading enzymes on the recombinant spore of Bacillus subtilis," *Biochem. Biophys. Res. Commun.*, vol. 510, no. 1, pp. 13–19, 2019, doi: 10.1016/j.bbrc.2018.12.077.

[62] P. Youngman, J. B. Perkins, and R. Losick, "Construction of a cloning site near one end of Tn917 into which foreign DNA may be inserted without affecting transposition in Bacillus subtilis or expression of the transposon-borne erm gene.," *Plasmid*, vol. 12, no.

1, pp. 1–9, Jul. 1984, doi: 10.1016/0147-619x(84)90061-1.

[63] H. AO, B. BW, R. K, and M. CP, "Characterization of cotJ, a sigma E-controlled operon affecting the polypeptide composition of the coat of Bacillus subtilis spores," *J. Bacteriol.*, vol. 177, no. 12, 1995, doi: 10.1128/JB.177.12.3394-3406.1995.

[64] D. Plácido, C. G. Fernandes, A. Isidro, M. A. Carrondo, A. O. Henriques, and M. Archer, "Auto-induction and purification of a Bacillus subtilis transglutaminase (Tgl) and its preliminary crystallographic characterization.," *Protein Expr. Purif.*, vol. 59, no. 1, pp. 1–8, May 2008, doi: 10.1016/j.pep.2007.12.004.

[65] K. M. Wiencek, N. A. Klapes, and P. M. Foegeding, "Hydrophobicity of Bacillus and Clostridium spores," *Appl. Environ. Microbiol.*, vol. 56, no. 9, pp. 2600–2605, 1990, doi: 10.1128/aem.56.9.2600-2605.1990.

[66] J. Sambrook and D. W. Russell, "Molecular cloning: a laboratory manual (3-volume set)," *Molecular cloning: a laboratory manual*. 2001.

[67] C. R. Harwood and S. M. Cutting, *Molecular biological methods for Bacillus*. 1990.

[68] Y. Zhang *et al.*, "Rapid Molecular Detection of SARS-CoV-2 (COVID-19) Virus RNA Using Colorimetric LAMP," *medRxiv*, p. 2020.02.26.20028373, Feb. 2020, doi: 10.1101/2020.02.26.20028373.

[69] C. B. F. Vogels *et al.*, "SalivaDirect: A simplified and flexible platform to enhance SARS-CoV-2 testing capacity.," *Med (New York, N.Y.)*, vol. 2, no. 3, pp. 263-280.e6, Mar. 2021, doi: 10.1016/j.medj.2020.12.010.

[70] Y. Ma, B. Zhang, M. Wang, Y. Ou, J. Wang, and S. Li, "Enhancement of Polymerase Activity of the Large Fragment in DNA Polymerase I from Geobacillus stearothermophilus by Site-Directed Mutagenesis at the Active Site.," *Biomed Res. Int.*, vol. 2016, p. 2906484, 2016, doi: 10.1155/2016/2906484.

[71] F. Wang, T. Song, H. Jiang, C. Pei, Q. Huang, and H. Xi, "Bacillus subtilis Spore Surface Display of Haloalkane Dehalogenase DhaA.," *Curr. Microbiol.*, vol. 76, no. 10, pp. 1161–1167, Oct. 2019, doi: 10.1007/s00284-019-01723-7.

[72] B. J, L. C. S, R. J, and M. T, "Sporobeads: The Utilization of the Bacillus subtilis Endospore Crust as a Protein Display Platform," *ACS Synth. Biol.*, vol. 7, no. 2, 2018, doi: 10.1021/ACSSYNBIO.7B00285.

[73] X. Chen, J. Zaro, and W.-C. Shen, "Fusion Protein Linkers: Property, Design and

Functionality," *Adv. Drug Deliv. Rev.*, vol. 65, no. 10, p. 1357, Oct. 2013, doi: 10.1016/J.ADDR.2012.09.039.

[74] R. Zilhão, M. Serrano, R. Isticato, E. Ricca, C. P. Moran, and A. O. Henriques, "Interactions among CotB, CotG, and CotH during assembly of the Bacillus subtilis spore coat.," *J. Bacteriol.*, vol. 186, no. 4, pp. 1110–9, Feb. 2004, doi: 10.1128/JB.186.4.1110-1119.2004.

[75] D. Imamura, R. Kuwana, H. Takamatsu, and K. Watabe, "Proteins Involved in Formation of the Outermost Layer of Bacillus subtilis Spores," *J. Bacteriol.*, vol. 193, no. 16, p. 4075, 2011, doi: 10.1128/JB.05310-11.

[76] M. T and Y. PC, "Western blot: technique, theory, and trouble shooting," *N. Am. J. Med. Sci.*, vol. 4, no. 9, 2012, doi: 10.4103/1947-2714.100998.

[77] P. Jockey, "Pipette Jockey," *MashUp-RT, purify your own reverse transcriptase*, 2018. https://pipettejockey.com/2018/09/06/mashup-rt-purify-your-own-reverse-transcriptase-beta-testing-phase/.

[78] N. E. BioLabs, "FAQ: Does Bst DNA polymerase have reverse transcriptase activity?," 2013. https://international.neb.com/faqs/2013/10/22/does-bst-dna-polymerase-have-reverse-transcriptase-activity.

[79] S. M. Monteiro, J. J. Clemente, A. O. Henriques, R. J. Gomes, M. J. Carrondo, and A. E. Cunha, "A Procedure for High-Yield Spore Production by Bacillus s ubtilis," *Biotechnol. Prog.*, vol. 21, no. 4, pp. 1026–1031, Sep. 2008, doi: 10.1021/bp050062z.

[80] Y. Su, C. Liu, H. Fang, and D. Zhang, "Bacillus subtilis: a universal cell factory for industry, agriculture, biomaterials and medicine," *Microb. Cell Fact.*, vol. 19, no. 1, p. 173, Dec. 2020, doi: 10.1186/s12934-020-01436-8.

[81] Y. Oh, J. A. Kim, C.-H. Kim, S.-K. Choi, and J.-G. Pan, "Bacillus subtilis spore vaccines displaying protective antigen induce functional antibodies and protective potency," *BMC Vet. Res.*, vol. 16, 2020, doi: 10.1186/S12917-020-02468-3.

[82] A. Rostami *et al.*, "Display of B. pumilus chitinase on the surface of B. subtilis spore as a potential biopesticide.," *Pestic. Biochem. Physiol.*, vol. 140, pp. 17–23, Aug. 2017, doi: 10.1016/j.pestbp.2017.05.008.

[83] H.-Y. Hsieh, C.-H. Lin, S.-Y. Hsu, and G. C. Stewart, "A Bacillus Spore-Based Display System for Bioremediation of Atrazine," *Appl. Environ. Microbiol.*, vol. 86, no. 18, 2020,

doi: 10.1128/AEM.01230-20.

[84] H. X, T. G, I. N, and W. X, "Developing RT-LAMP assays for rapid diagnosis of SARS-CoV-2 in saliva," *EBioMedicine*, vol. 75, 2022, doi: 10.1016/J.EBIOM.2021.103736.

[85] M. Soroka, B. Wasowicz, and A. Rymaszewska, "Loop-Mediated Isothermal Amplification (LAMP): The Better Sibling of PCR?," *Cells*, vol. 10, no. 8, p. 1931, Jul. 2021, doi: 10.3390/cells10081931.

[86] H. Wang, R. Yang, X. Hua, W. Zhao, and W. Zhang, "Functional display of active β-galactosidase on Bacillus subtilis spores using crust proteins as carriers," *Food Sci. Biotechnol.*, vol. 24, no. 5, pp. 1755–1759, Oct. 2015, doi: 10.1007/s10068-015-0228-3.

[87] J. Bartels, S. López Castellanos, J. Radeck, and T. Mascher, "Sporobeads: The Utilization of the Bacillus subtilis Endospore Crust as a Protein Display Platform," *ACS Synth. Biol.*, vol. 7, no. 2, pp. 452–461, 2018, doi: 10.1021/acssynbio.7b00285.

[88] K. B. Nguyen *et al.*, "Phosphorylation of spore coat proteins by a family of atypical protein kinases.," *Proc. Natl. Acad. Sci. U. S. A.*, vol. 113, no. 25, pp. E3482-91, 2016, doi: 10.1073/pnas.1605917113.

[89] S. Mingmongkolchai and W. Panbangred, "Display of Escherichia coli Phytase on the Surface of Bacillus subtilis Spore Using CotG as an Anchor Protein," *Appl. Biochem. Biotechnol.*, vol. 187, no. 3, pp. 838–855, Mar. 2019, doi: 10.1007/s12010-018-2855-7.

[90] G. C, H. M, H. CR, and E. T, "Extracellular Self-Assembly of Functional and Tunable Protein Conjugates from Bacillus subtilis," *ACS Synth. Biol.*, vol. 6, no. 6, 2017, doi: 10.1021/ACSSYNBIO.6B00292.

[91] B. CN *et al.*, "Genetically Encoded Spy Peptide Fusion System to Detect Plasma Membrane-Localized Proteins In Vivo," *Chem. Biol.*, vol. 22, no. 8, 2015, doi: 10.1016/J.CHEMBIOL.2015.06.020.

[92] G. Wang, X. Ding, J. Hu, W. Wu, J. Sun, and Y. Mu, "Unusual isothermal multimerization and amplification by the strand-displacing DNA polymerases with reverse transcription activities," *Sci. Rep.*, vol. 7, no. 1, p. 13928, Dec. 2017, doi: 10.1038/s41598-017-13324-0.

[93] C. Shi, X. Shen, and S. Niu, "Innate Reverse Transcriptase Activity of DNA Polymerase for Isothermal RNA Direct Detection," pp. 13804–13806, 2015, doi: 10.1021/jacs.5b08144.

Chapter 6 – Annex

Annex 6.1- Bacterial strains used in this study

Strain	Relevant Proprieties	Origin
E. coli		
DH5α	F– Φ80l*acZ*ΔM15 Δ(*lacZYAargF*) *U169 recA1 endA1 hsdR17* (rK–, mK+) *phoA supE44 λ– thi-1 gyrA96 relA1*	Invitrogen
BL21	F- *ompT gal dcm Ion hsdSB* (*rB-mB-)* λ (DE3 [*lacI lac UV5-T7p07 ind1 sam7 nin5]*) [*malB*+]K-12 (λS)	Novagen
MSE50	BL21 containing pET28+BstI, Kan^R	[57]
B. subtilis		
PY79	Prototrophic derivative of *B. subtilis* 168	[62]
MSB250	*cotZΩcotZ-lk-bst-his*,Cm^R	This study
MSB251	*amyE*::P_{cotYZ}- *cotY-lk-bst-his*, Cm^R	“
MSB252	*amyE*::P_{cotYZ} *-his-bst-lk-cotY*, Cm^R	“
MSB253	*amyE*::P_{cotYZ} *-his-FeLRT-lk-cotY*, Cm^R	“
MSB254	*cotZΩcotZ-lk-FeLRT-his*, Cm^R	“
MSB255	*cotZΩcotZ-lk-bst*, Cm^R	“

Annex 6.2- Oligonucleotides used in this study

Primer	Sequence (5' to 3')[a]
CotZ_Fw_HindIII	CCCAAGCTTTCGTTAGGCGACACAGTGCC
Bst_SOE_Lk_Fw_CotZand CotY_Bst	GCTGCAGCGAAGGCTGCAGCGGAGGGTGAAA AACCGCTGG
Lk_SOE_Bst_Rev_CotZand CotY_Bst	CCAGCGGTTTTTCACCCTCCGCTGCAGCCTTCG CTGCAGC
Bst_6XHis_Rev_BamHI	GCGGGATCCTTAGTGGTGGTGGTGGTGGTGCT TCGCATCGTACCAGGTCG
Quickchange_Fw	CCTGGTACGATGCGAAG**TAA**CACCACCACCAC CAC
Quickchange_Rev	GTGGTGGTGGTGGTG**TTA**CTTCGCATCGTACC AGG
Bst_Fw_XbaI	CGGTCTAGAAGGAGGTCGCGGCATGCACCACC ACCACCACCACGAGGGTGAAAAACCGCTGG
Lk_SOE_Bst_Fw_Bst_Cot Y	CCGACCTGGTACGATGCGAAGCTGGGCGGAG GCGGATCAGG
Bst_SOE_Lk_Rev_Bst_Cot Y	CCTGATCCGCCTCCGCCCAGCTTCGCATCGTA CCAGGTCGG
LK_rev_NgoMIV	ACGGCCGGCCGCTGCAGCCTTCGCTGCAGCC
LK_Fw_AgeI	TCGACCGGTCTGGGCGGAGGCGGATCAG
Bst_Rev_SpeI	CTGACTAGTATTAGTGGTGGTGGTGGTGGTGC TTCGCATCGTACCAGGTC
XbaI_FeLRT_FW	CGGTCTAGAAGGAGGTCGCGGCATGCACCACC ACCACCACCACACCCTGCAGCTGGAAGAAG
SOE_FeLRT_Lk_Fw	CCAGTCTTCTCTGACCATCAACCTGGGCGGAG GCGGATCAGG
SOE_LK_FeLRT_Rev	CCTGATCCGCCTCCGCCCAGGTTGATGGTCAG AGAAGACTGG
NgoMIV_Lk_Rev	ACGGCCGGCCGCTGCAGCCTTCGCTGC
SOE_FeLRT_Fw_Z	GCAGCGAAGGCTGCAGCGACCCTGCAGCTGG AAGAAG
SOE_FeLRT_Rev_Z	CTTCTTCCAGCTGCAGGGTCGCTGCAGCCTTC GCTGC

FeLRT_Rev_Z	GCGGGATCCTTAGTGGTGGTGGTGGTGGTGGT TGATGGTCAGAGAAGAC
Ca_F3	TCTGGTATTCCGGAGGGC
Ca_B3	AGTCCTACCTGATTTGAGGT
Ca_FIP	CTACCGTCTTTCAAGCAAACCCATGAGCGTCG TTTCTCCCT
Ca_BIP	TTGACAATGGCTTAGGTCTAACCAAAAGATAA CGTGGTGGACGTTAC
Ca_LB	CTCAACACCAAACCCAGCGG
SARS_F3	TGGCTACTACCGAAGAGCT
SARS_B3	TGCAGCATTGTTAGCAGGAT
SARS_FIP	TCTGGCCCAGTTCCTAGGTAGTCCAGACGAAT TCGTGGTGG
SARS_BIP	AGACGGCATCATATGGGTTGCACGGGTGCCAA TGTGATCT
SARS_LF	GGACTGAGATCTTTCATTTTACCGT
SARS_LB	ACTGAGGGAGCCTTGAATACA
N1_F	GACCCCAAAATCAGCGAAAT
N1_R	TCTGGTTACTGCCAGTTGAATCTG

[a)] restriction sites are underlined; base substitutions are shown in bold.

Annex 6.3- Plasmids used in this study

Plasmid	Relevant Proprieties	Origin
pMS38	pLitmus29 derivative with a chloramphenicol resistance cassette, Amp^R Cm^R	[74]
p1CSV-CotY-N	*amy*E::PcotYZ-*cotY-rfp cat*, Amp^R Cm^R	[72]
p1CSV-CotY-C	*amy*E::PcotYZ-*rfp-cotY cat*, Amp^R Cm^R	"
pBst	$pET28^+$ carrying *bst*, Amp^R	[57]
MashUp RT	Plasmid carrying a modified Feline Leukemia Virus Reverse Transcriptase, Kan^R	[77]
pCN01	*cotZ-lk-bst-his* in pMS38	This study
pCN02	*lk-bst-his* in p1CSV-CotY-C	"
pCN03	*his-bst-lk* in p1CSV-CotY-N	"
pCN04	*his-FeLRT-lk* in p1CSV-CotY-N	"
pCN05	*cotZ-lk-FeLRT-his* in pMS38	"
pCN06	*cotZ-lk-bst* in pMS38	"

Annex 6.4- Growth Media

Solution	Composition (for 1 L)
Auto-induction medium	1 mL 1M $MgSO_4$; 20 mL 50x5052; 50 mL 20xNPS; 929 mL LB medium
Luria Broth (LB)	10 g tryptone; 5 g yeast extract; 5 g NaCl
Luria Agar (LA)	10 g tryptone; 5 g yeast extract; 5 g NaCl; 16 g agar
Difco Sporulation Medium (DSM)	8 g nutrient broth; 1 g KCl, 0.25 g $MgSO_4.7H_2O$ or 0.12 g $MgSO_4$
Growth Media 1 (GM1)	960 mL B&W salts; 10 mL 100 mM $MgSO_4$; 10 mL 50% glucose; 10 mL 10% yeast extract; 10 mL B&W Aminoacids 5X
Growth Media 2 (GM2)	965 mL GM1; 5 mL 50 mM $CaCl_2$; 25 mL 1 M $MgCl_2$

Annex 6.5- Solutions and Buffers

Solution	Composition (100 mL)
Bott & Wilson salts (B&W salts)	1.24 g K_2HPO_4; 0.76 g KH_2PO_4; 0.1 g tri-sodic citrate; 0.6 g $(NH_4)_2SO_4$
B&W amino acids 5X	250 mg Trp, Arg, Lys, Gly, Met, His, Val, Thr, Asp
Blocking solution	5% (w/v) powder skin milk diluted in PBS-Tween
Buffer A	150 mM NaCl; 50 mM Tris–HCl pH 7.5
Buffer B	Bufer A with 0.5 M Imidazol
1x master mix	10 mM $(NH_4)_2SO_4$; 50 mM KCl; 8 mM $MgSO_4$; 0.1% Tween 20; 1.4 mM each dNTP
French Press Buffer	10 mM Tris; pH 8; 10 mM $MgCl_2$; 0.5 Mm EDTA; 0.2 M NaCl; 10% glycerol; 0.1 mM DTT
LAMP 2x Reaction Buffer	40 mM Tris–HCl (pH 8.8); 20 mM KCl; 20 mM $(NH_4)_2SO_4$; 16 mM $MgSO_4$; 0.2% Tween 20
Orange G	0.2% orange G; 0.37% EDTA; 50% glycerol
PBS 10X	137 mM NaCl; 2.7 mM KCl; 4.3 mM Na_2HPO_4; 1.4 mM KH_2PO_4
PBS-Tween	10 mL PBS 10X; 0.1 mL Tween 20
Revolving gel	4.5% acrylamide (29:1); 0.375 M Tris.Cl; 0.1% SDS pH 8.8; 0.8% APS and 10% (v/v) TEMED
Staking gel	4.5% acrylamide (29:1); 0.125 M Tris.Cl; 0.1% SDS pH 6.8; 0.01% APS and 10% (v/v) TEMED
SDS-Page Loading Buffer	1x Upper Tris; 5%Glycerol; 2% (w/v) SDS; 0.5 mM DTT; 5% 2-mercaptoetano; 0.025% (w/v) bromophenol blue
STET Buffer	8% sucrose; 0.5% TritonX-100; 50 mM EDTA; 10 mM Tris-HCl pH 8
Coomassie solution	0.5 g/mL Coomassie Brilliant Blue R-250; 80% absolute ethanol; 20% acetic acid
Destaining solution	30% absolute ethanol; 10% acetic acid
TAE 1x	40 mM Tris; 20 mM acetic acid; 1 mM EDTA

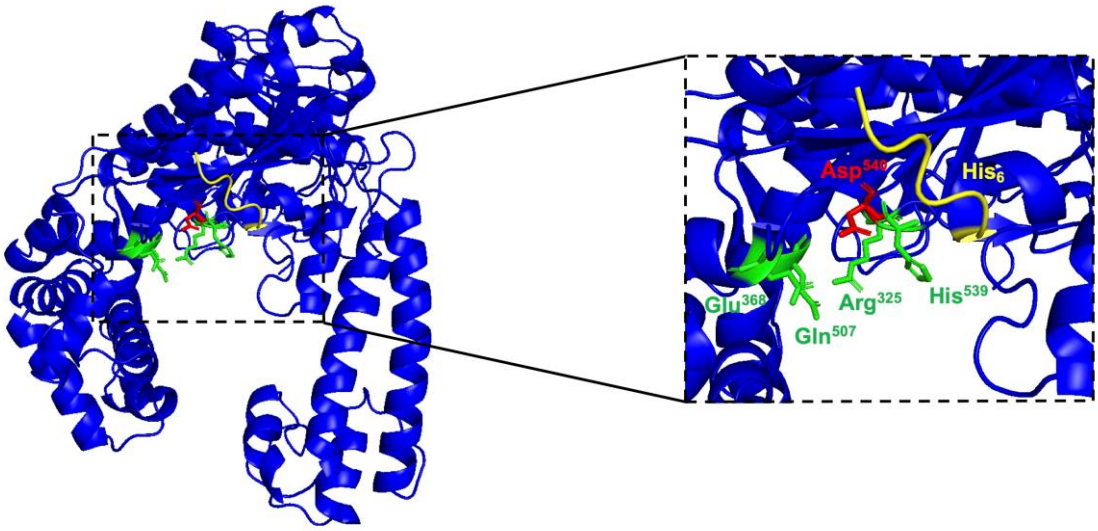

Annex 6.6. The structure of Bst polymerase. The left panel shows the structural model for the Bst polymerase. The active site of Bst is highlighted in the square and expanded on the right. The active site of the Bst is formed by the amino acid residues Arg325, Glu368, Gln507, His539 and Asp540. Asp540 is responsible for the formation of a hydrogen bond with the nucleotides and interacts with the Mg^{2+} ion. Although in a flexible region of the protein, the His_6 tag (in yellow) appears to be close to the active site of the enzyme, obstructing the entry of new nucleotides.